CDF/PUB/CALORIMETRY/PUBLIC/5669
Version 1.0
June 29, 2001

PMT Linearity Test

Howard Budd, University of Rochester
Hongquan Niu, Brandeis University

Abstract

The linearities of the CDF PMTs are tested using the apparatus described in Reference [1]. The light source is generated by a laser shining on a wave-shifting dye. The dye light shines on both a pin diode which is read out with a 20-bit Burr-Brown ADC and a lens which focuses the light into the quartz fiber. The quartz fiber brings the light to a wave-shifter (BBQ) in a light tight box. The wave-shifter absorbs and re-emits the light in all directions. The re-emitted light shines on the PMT which is being tested. The signal from the PMT is read out using the QIE electronics. We test a small sample of tubes from each CDF calorimeter. We conclude the following (at equivalent energy scale of 200 GeV in the worst case): The PEM tube has nonlinearity less than 2.0%, the PHA tube has nonlinearity less than 1.5%, the CEM tube has nonlinearity less than 3.0%, the CHA tube has nonlinearity less than 4.0%, and the WHA tube has nonlinearity less than 6.0%.

1 Linearity test apparatus

1.1 The apparatus

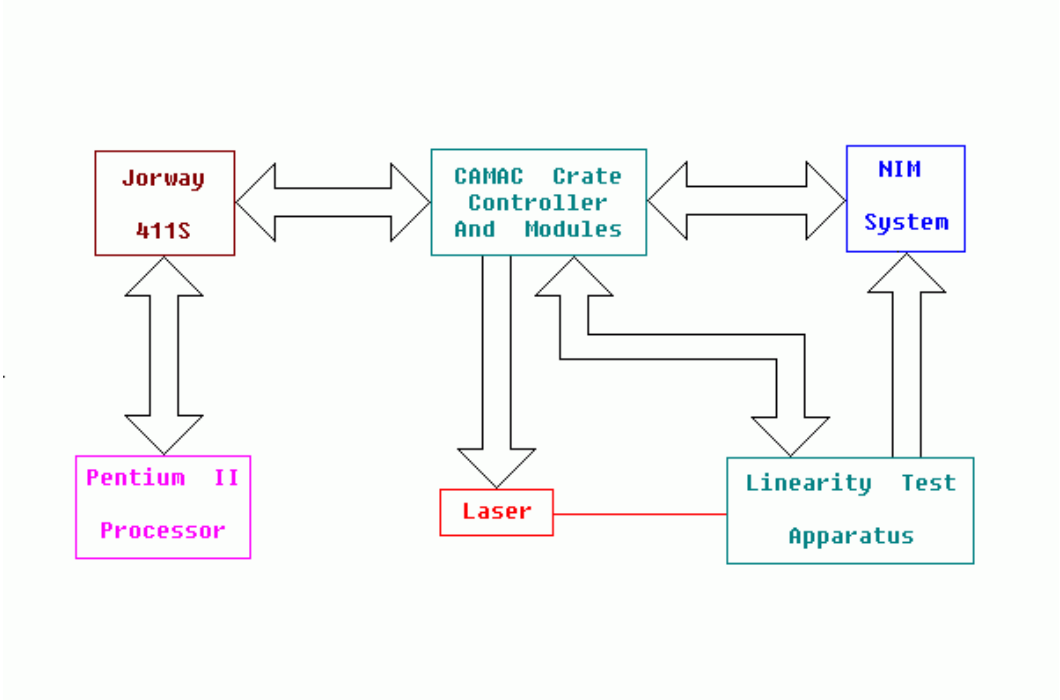

Figure 1: Overview of the PMT linearity test setup

We use the same "PMT linearity test setup" described in QIE Linearity Test [1] to test the PMT, except we bring the light to a PMT instead of pin diode. Reference [1] describes the PMT linearity test system. We only state the relevant information in this document.

Figure 1 gives an overview of the PMT linearity test setup. Figure 2 shows the Linearity Test Apparatus. The electronics are controlled with a CAMAC and NIM system connected to a 200 MHz Pentium processor using the Redhat LINUX operating system. The CAMAC library is LINUX SJY v1.0, downloaded from the Fermilab Computing Division [2]. An Adaptec 2940 SCSI bus host adapter is installed in the PC using the aic7xxx driver distributed with LINUX 2.0.29. The information and commands are trans-

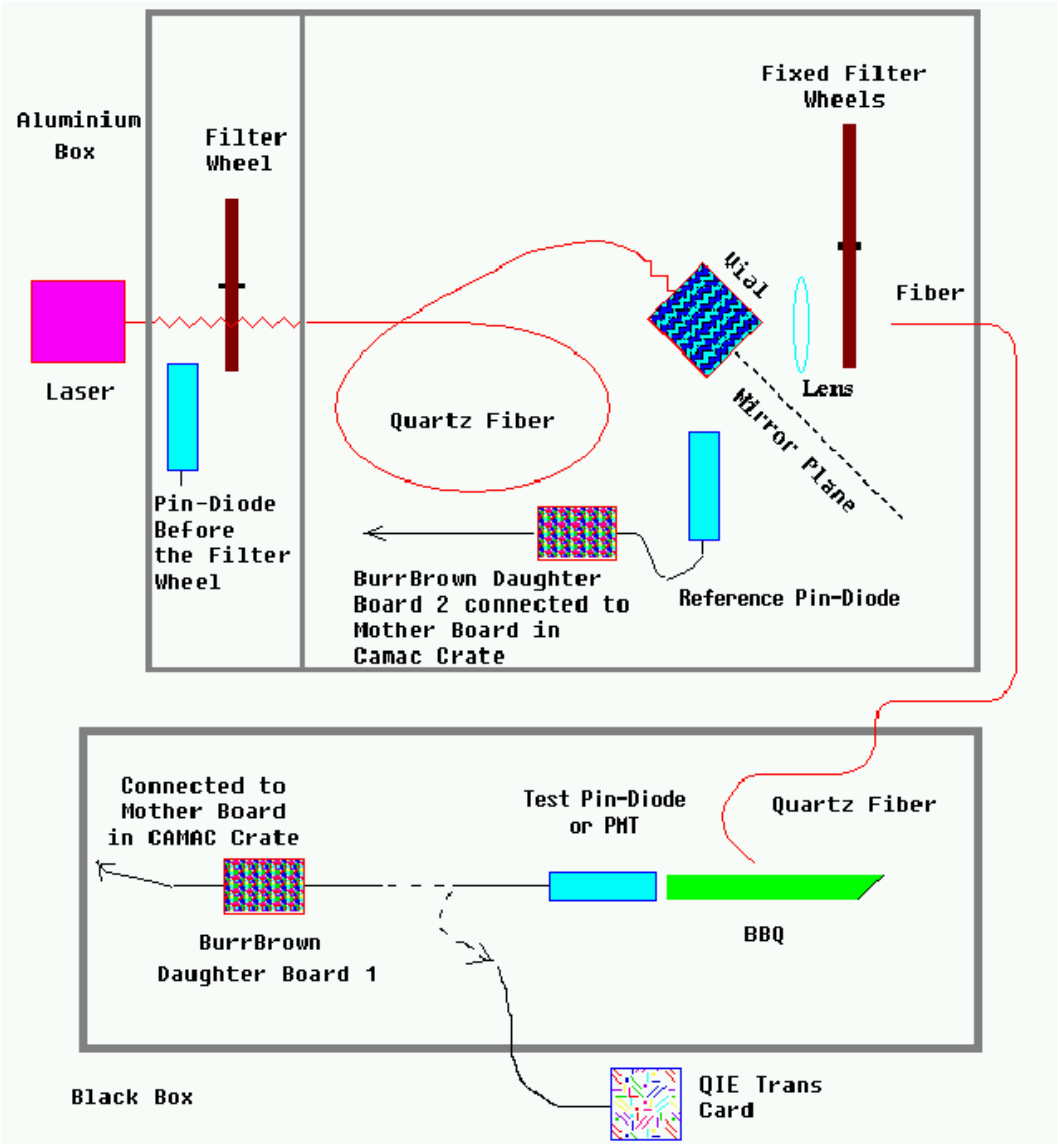

Figure 2: Linearity Test Apparatus

ferred between the PC and the CAMAC system using the Jorway 411S CAMAC Highway Driver.

The reference ADC is the high resolution DDC101 Burr-Brown ADC. The Burr-Brown ADC has 20-bit resolution (0.5fc/count) with an advertised integral nonlinearity of 0.003%

over the full scale range[3]. The system is read out using CAMAC with the mother card in the CAMAC create. The mother card reads out two daughter cards. The daughter card contains a Burr-Brown ADC which is connected to the pin diode via a short cable.

The setup uses 2 pin diodes. One pin diode is called the Reference Pin-Diode, and the other one is called the Test Pin Diode. These two pin diodes have identical constructions. The Reference Pin-Diode is positioned in the Aluminum Box for the purpose of giving a linear reference for the tested PMT. The Test Pin-Diode is placed in the Black Box for the purpose of testing the optical linearity of the setup. The Black Box is a specially made light tight box for testing the PMT, see Figure 2.

The light intensity from the laser is controlled using a rotating filter wheel. The rotation of the filter wheel works in the so called "step mode". That is, the wheel rotates to a fixed angle and stops. The laser fires at 5 Hz for a fixed number of times. Then, the wheel rotates to another angle, and the laser fires again. In such mode, we have discrete points with a smaller statistical error for each point, and we can give a statistical error for each point.

The laser light passes through the filter wheel to a quartz fiber. The fiber injects the light into the center of a small square vial containing dye (sodium salicylate dissolved in ethanol). The dye re-emits light in all directions.

The light from the dye is measured by the reference system and the PMT. The light is not emitted uniformly around the dye box, but the light is mirror symmetric about the plane of the light hitting the dye box. The Reference Pin Diode and the dye light collection lens sit in symmetric positions about the mirror plane. Since they are at symmetric positions, the amount of light they collect are proportional to each other. As the filter wheel rotates, the ratio of the light reaching the Reference Pin Diode and the lens stays constant.

The lens focuses the dye light onto a quartz fiber. The focused dye light passes through two sets of fixed filter wheels and hits the fiber. These two sets of fixed filter wheels are controlled by the software to attenuate the light from the dye to the quartz fiber by rotating the wheel so different filters are between the dye and the quartz fiber. We can achieve the transmission constant from 1 to 1.35×10^{-5} by rotating these filter wheels. Thus we can adjust the light intensity according to the gains of the different tubes, and we can study different ranges of a tube.

The quartz fiber brings the dye light to a wave-shifter(BBQ) inside the Black Box. The wave-shifter absorbs and re-emits the light into all directions again. The quartz fiber

points away from the PMT so that only wave-shifted light reaches the PMT. No unshifted light from the quartz fiber reaches the PMT. The wave-shifted light is measured by the PMT. The PMT is read out with the QIE electronics. We can also put the Test Pin Diode inside the Black Box to test the setup's optical nonlinearity. The quartz fiber is pointed directly at the Test Pin Diode without BBQ to test the linearity of the system.

The QIE electronics is CDF Run II calorimetry electronics[4]. It runs with a 132 ns clock, and integrates the signal in each clock cycle. The QIE electronics reads out four consecutive time slices of integration. The four consecutive time slices are also called four buffers.

1.2 Shape of the PMT signals

The linearity of the PMT is a function of the peak current. Hence we must wave-shift the dye light so the shape of the light reaching the PMT matches the shape of the pulse from the calorimeters. Figure 3 shows the shape of the signal from the dye light measured by the PLUG tube. The FWHM for this signal is 11 ns which is much shorter than the test beam pulse. Figures 4 and 5 show examples of what the test beam signals look like. Reference [5] shows the test beam signals for all the calorimeter, CHA, CEM, PEM, PHA and WHA. In order to match the test beam pulses the dye light is wave-shifted using a piece of BBQ. The quartz fiber is directed at the piece of BBQ, but away from the PMT. This ensures the PMT only sees shifted light. Figure 6 shows that the shape of the shifted light for the PLUG tube is similar to the test beam pulse. The FWHM is 20 ns, and the test beam pulses are 20 ns FWHM. We use BBQ to shift the light for all the tubes. We do the same to the other type of tubes as well. See the figures 7 - 9.

The WHA tube signal FWHM for the BBQ signal varies, mostly between 20 ns and 25 ns. The signal FWHM from some of the low voltage WHA tubes are as wide as 32 ns for high laser light. The high intensity of the light widens the signal shape. The wider signal shape may be related to the worse nonlinearity of the WHA tubes.

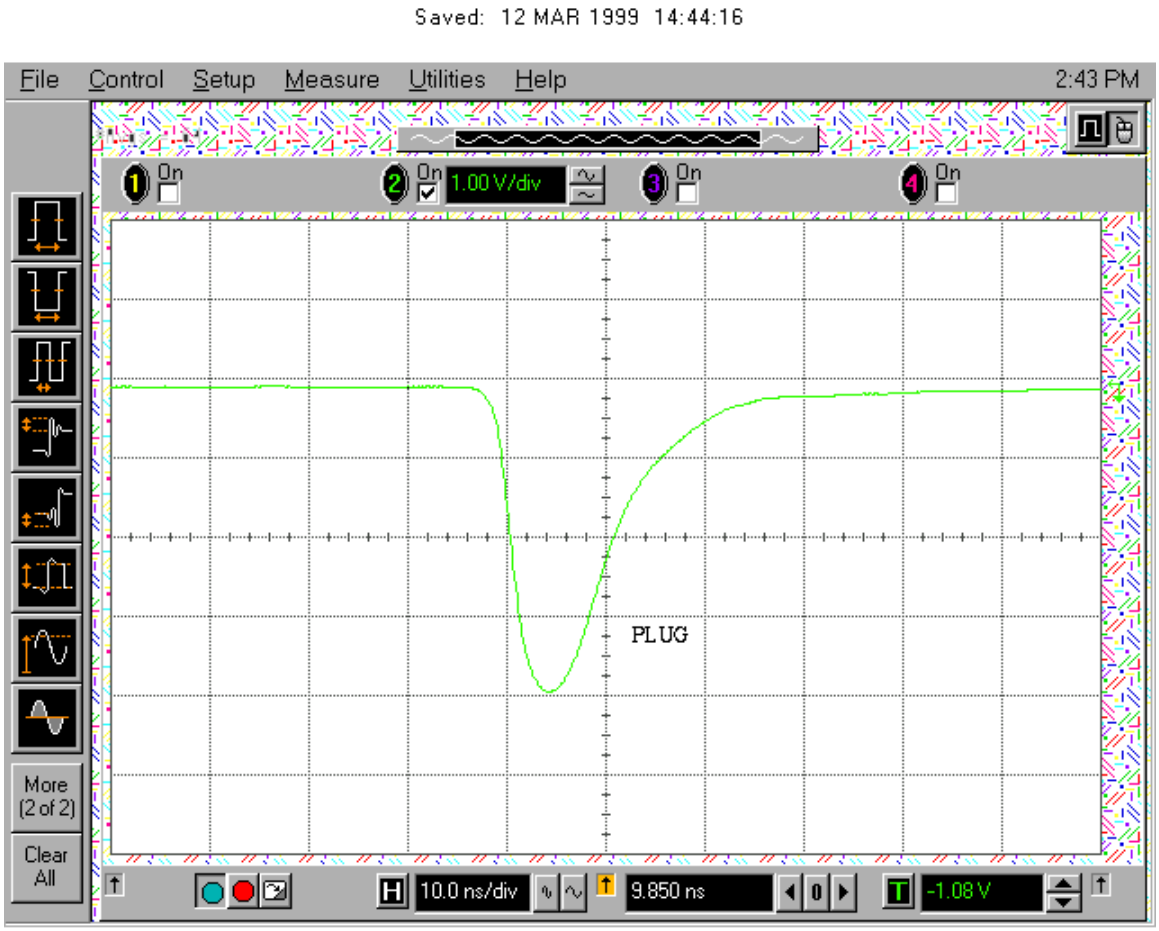

Figure 3: Plug tube signal when the quartz fiber is directly pointed at the tube. The FWHM is 11 ns.

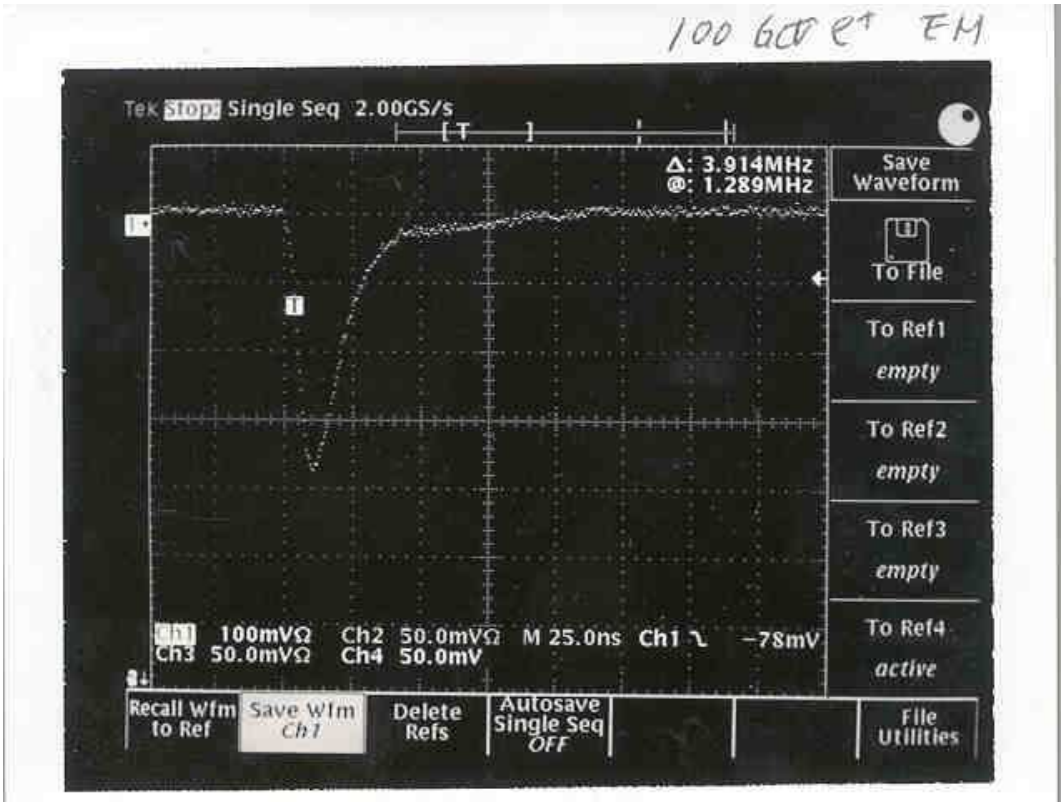

Figure 4: An example of the Plug EM testbeam signal. The FWHM is 20 ns.

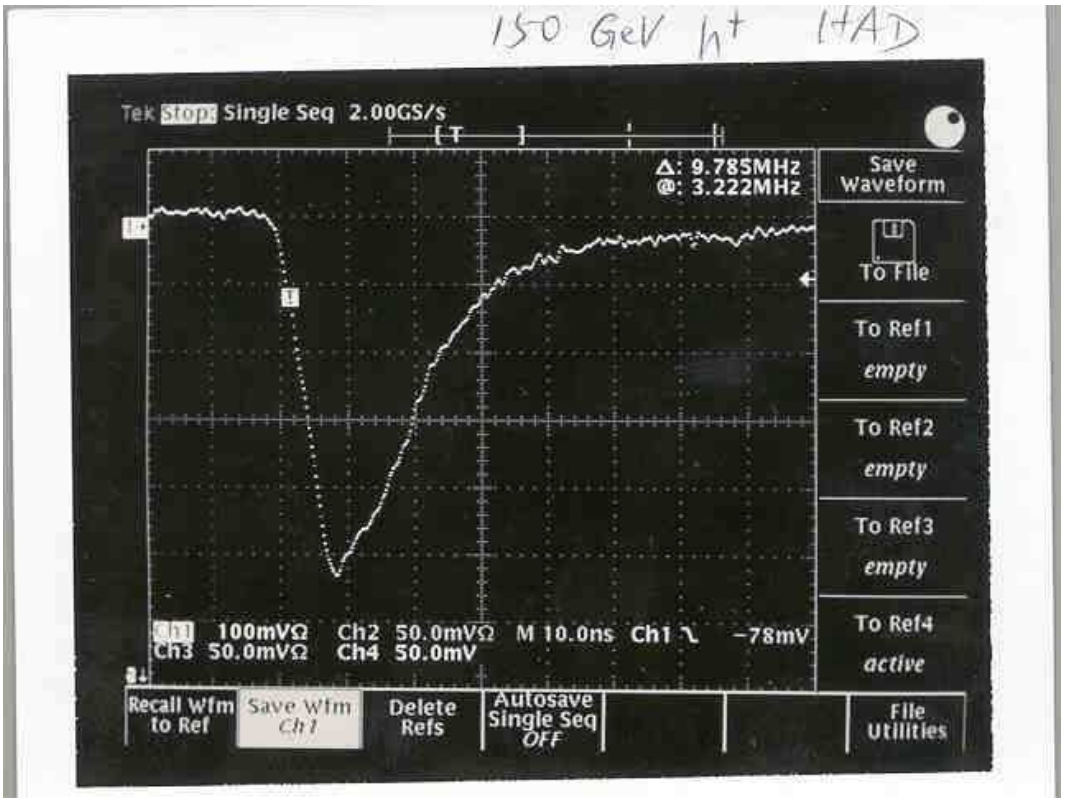

Figure 5: An example of the Plug HA testbeam signal. The FWHM is 20 ns.

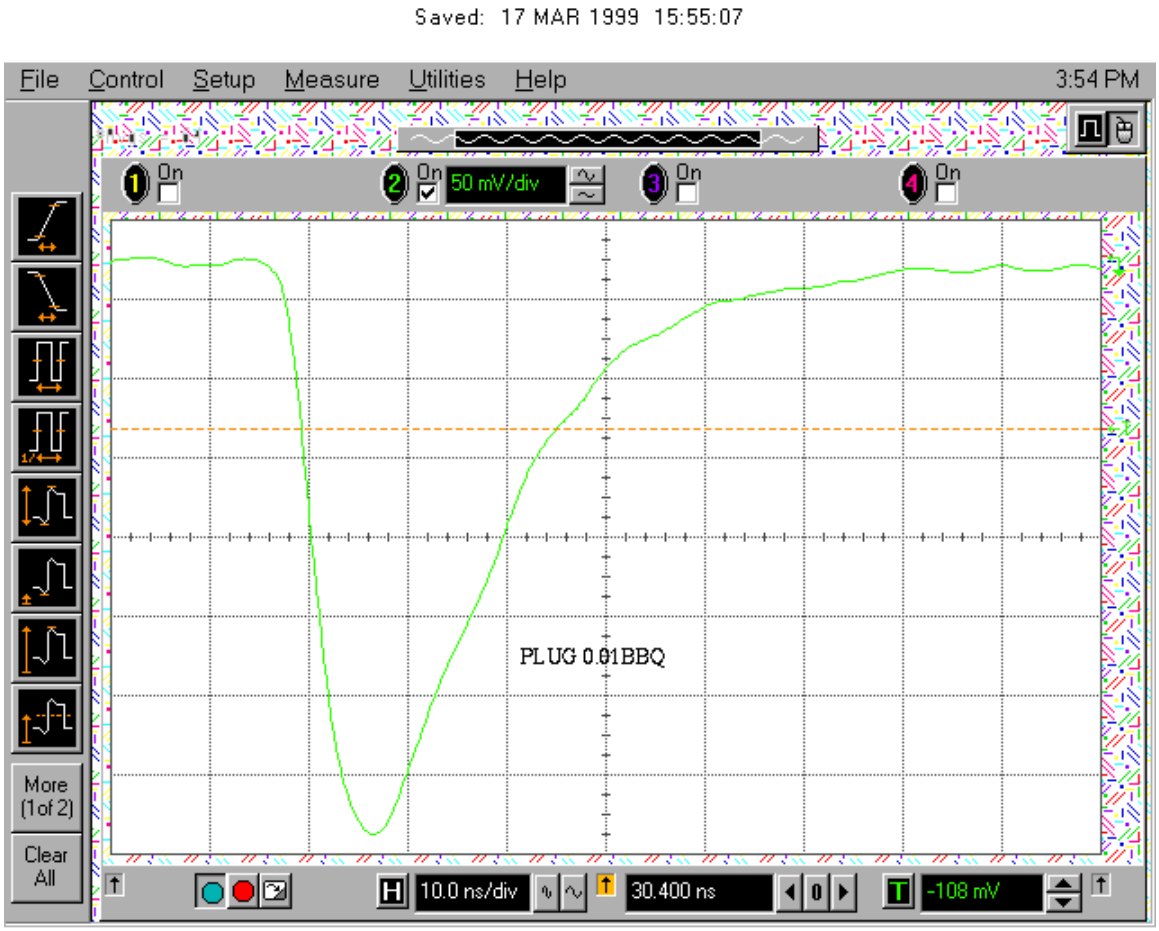

Figure 6: Plug tube signal when the quartz fiber is directed at a piece of BBQ, but away from the PMT. The FWHM is 20 ns.

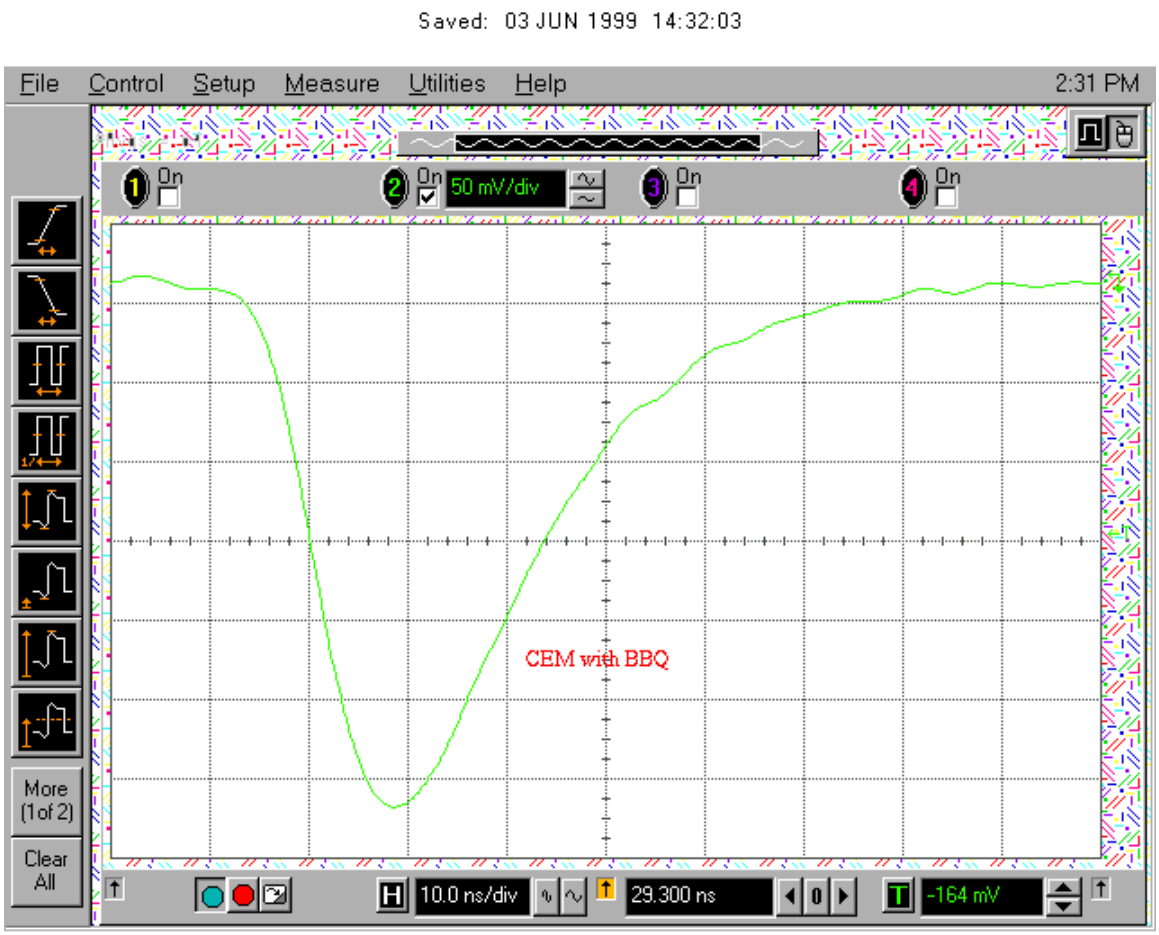

Figure 7: CEM tube signal when the quartz fiber is directed at a piece of BBQ, but away from the PMT. The FWHM is 24 ns.

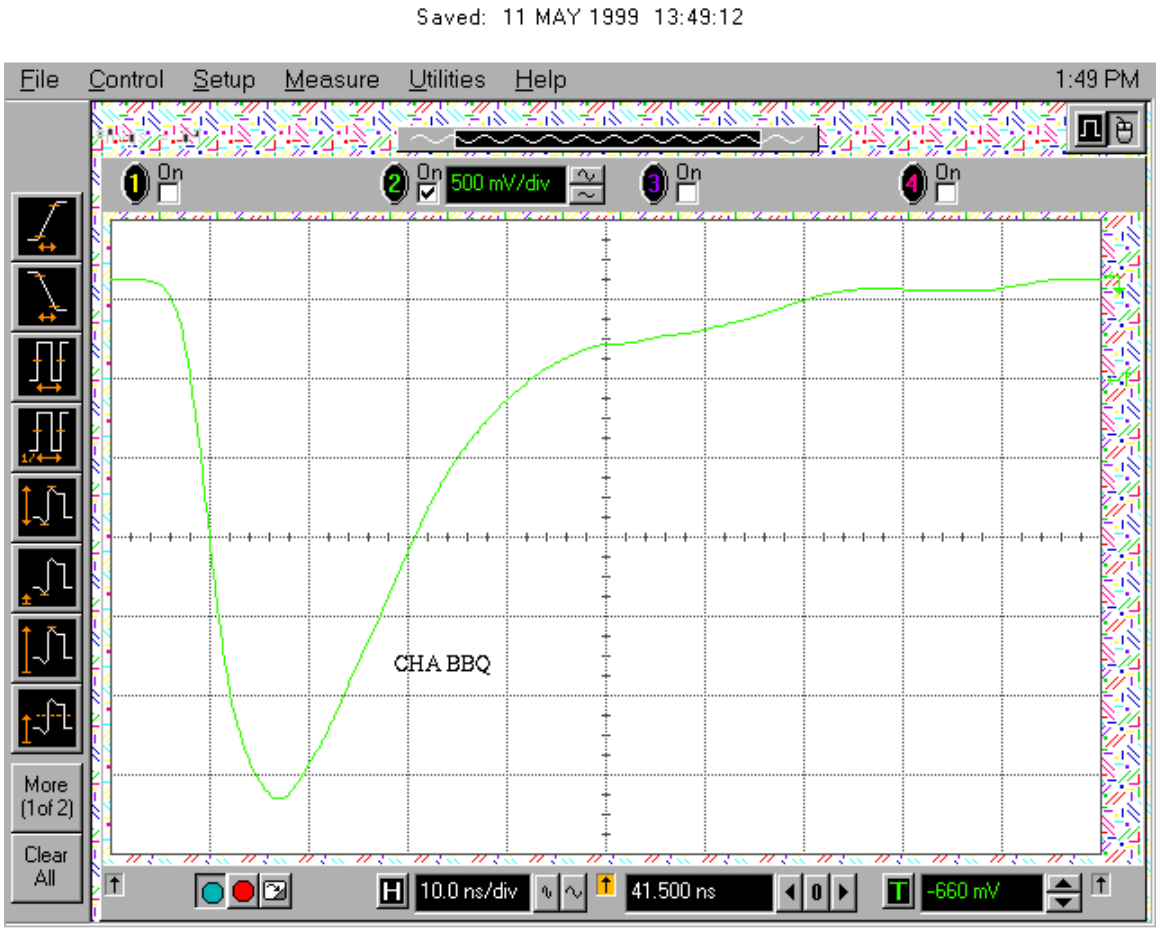

Figure 8: CHA tube signal when the quartz fiber is directed at a piece of BBQ, but away from the PMT. The FWHM is 21 ns.

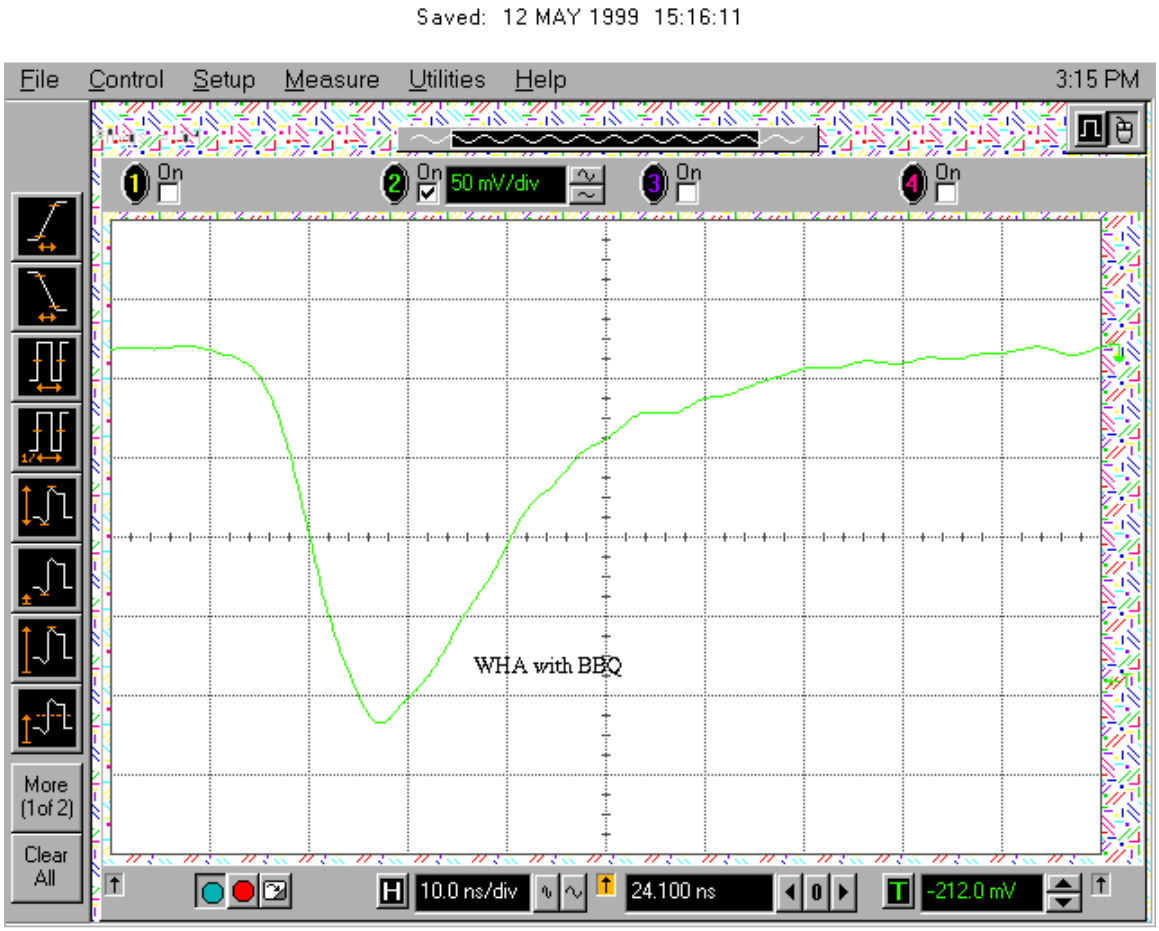

Figure 9: WHA tube signal when the quartz fiber is directed at a piece of BBQ, but away from the PMT. The FWHM is 20 ns.

1.3 Test of the linearity test apparatus

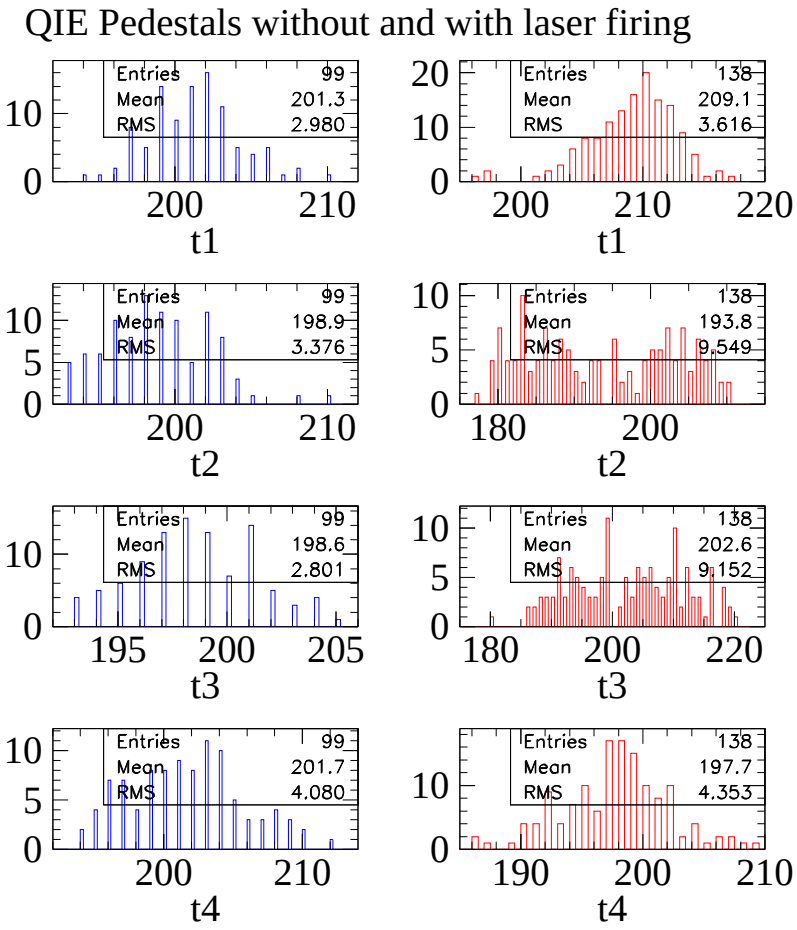

Figure 10: Pedestals of PLUG tube. The left hand side is pseudo pedestals(without laser firing) for 4 QIE buffers. The right hand side is laser pedestals(with laser firing but but with no light reaching the PMT) for 4 QIE buffers. The pseudo-pedestals and laser pedestals for the 4 buffers are different.

The laser firing generates noise we call "laser noise". The PMT sees the laser noise while the pin diodes do not see the laser noise.

The pedestal is measured for each run by gating the ADCs without firing the laser. The

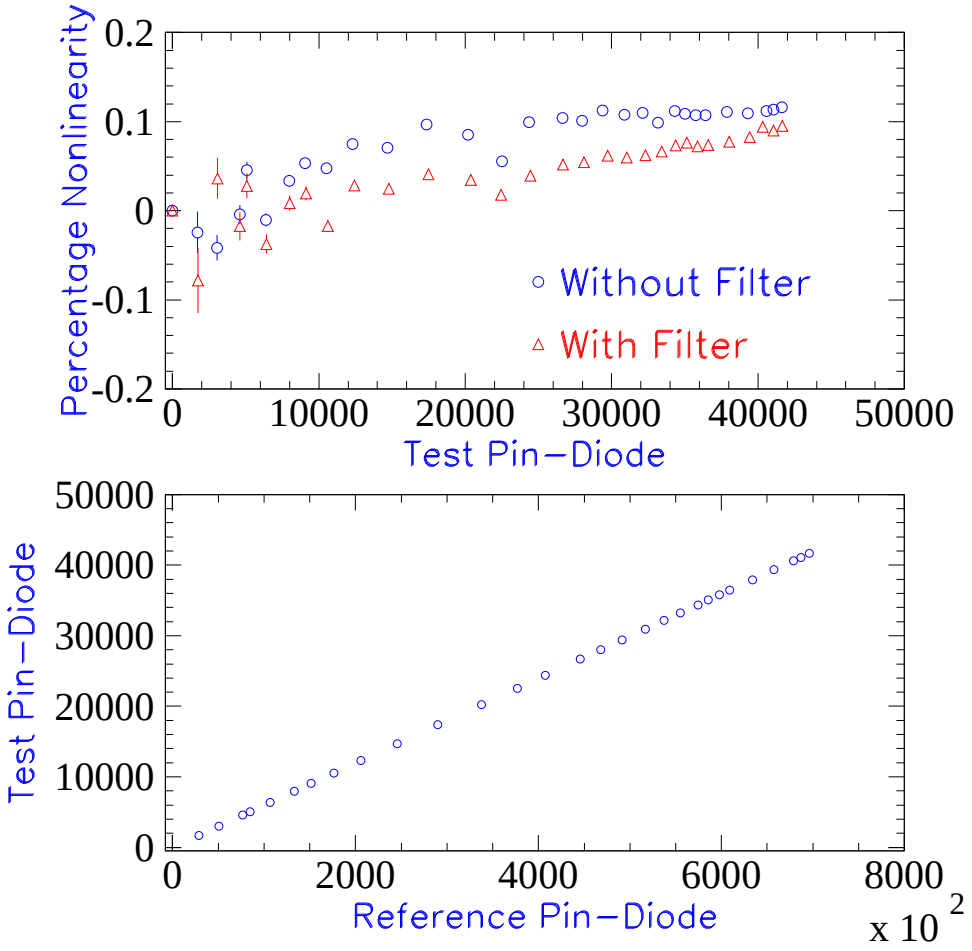

Figure 11: Linearity of the apparatus without BBQ. The quartz fiber points at the test pin diode in the Black Box. It shows the optical linearity of the setup. The plot on the top is percentage nonlinearity of the Test Pin-Diode with and without a neutral density filter before the Reference Pin-Diode. This is to test the linearity effect of the filter. The plot on the bottom is the Test Pin-Diode counts vs Reference Pin-Diode counts. The Pin-Diode counts are Burr-Brown counts.

"real" pedestal should be measured when the laser is firing, but with no light reaching either the PMT or the reference pin diode. The PMT pedestals are set to 200 counts

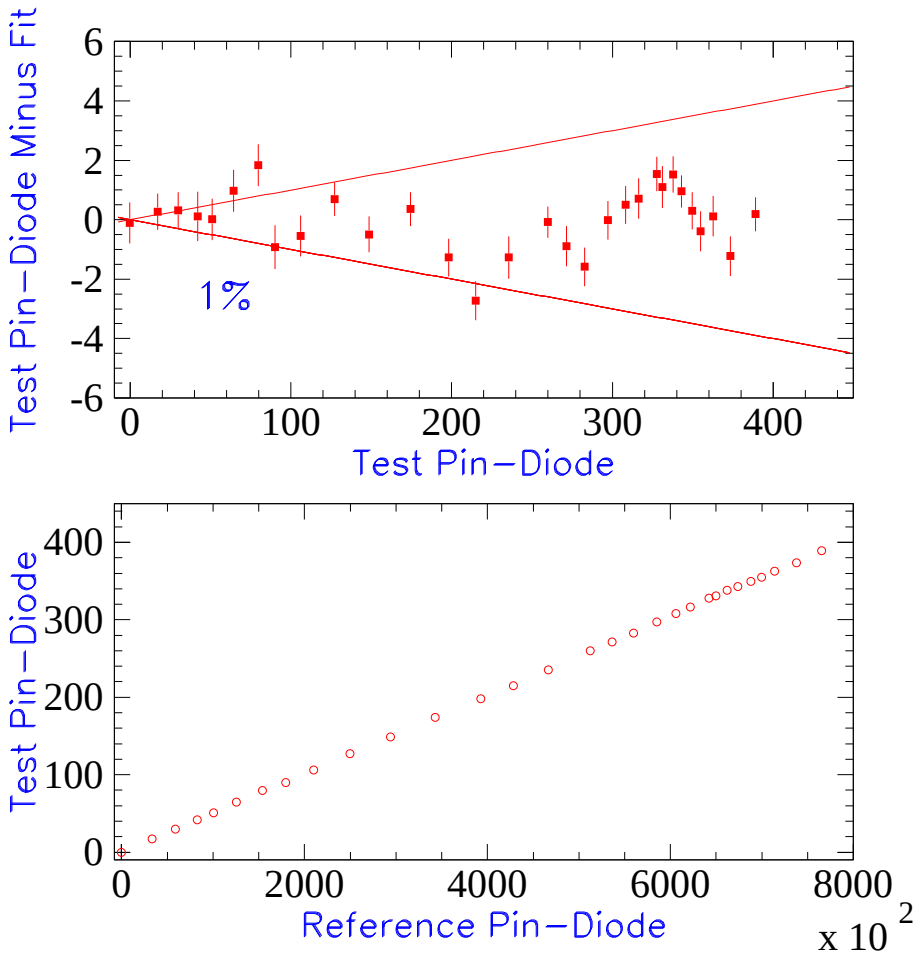

Figure 12: Linearity of the apparatus with BBQ. The quartz fiber points away from the Test Pin-Diode at a small bar with BBQ. The Test Pin-Diode reads out shifted light. The plot on the top is the Test Pin-Diode counts minus the fitted value vs Test Pin-Diode counts. The 1% line is also drawn on the same plot. The plot on the bottom is the Test Pin-Diode counts vs Reference Pin-Diode. All the Pin-Diode counts are Burr-Brown counts. It tests for any saturation effect in the BBQ.

for each buffer by software. We define "laser pedestal" as the measured pedestal when the laser is firing and the quartz fiber to the dye is taped off. The "pseudo pedestal" is

measured when there is no laser firing. Of course, laser pedestal cannot be taken during a linearity run. The difference between laser pedestal and pseudo pedestal is due to the laser noise. We can adjust the pseudo pedestal to laser pedestal by adding the average difference between laser pedestal and pseudo pedestal. We have worked to make the difference as small as possible.

Because of the PLUG tubes have very long wires, they picks up much more laser noise than the other type of the tubes. We reduce the noise by carefully positioning the wires in the Black Box. If we sum buffer 2 and buffer 3, the noise cancels each other and makes the difference smaller, typically around -1 and -2 counts. Here, the minus sign means the average of the laser pedestal is less than the average of the pseudo pedestal. If we only use buffer 2, the difference can be larger. For the PLUG tubes, it can be as large as -10 counts and it various from tube to tube. We use buffer 2 only through out our note. This won't affect the high end of our PMT linearity test results. But for the low end, it does have some effects. We also have separate ASCII files which contain the test result for both buffer 2 only and sum of buffer 2 and buffer 3.

We test the linearity of the system. We put the Test Pin Diode in the Black Box and position the fiber directly onto the Test Pin Diode. After the Reference Pin Diode is carefully positioned opposite the lens on the mirror plane, we achieve optical nonlinearity $< 0.15\%$. Throughout the PMT linearity test we use a neutral density filter before the lens to adjust the laser light level. We set the highest laser light level so that it just starts to saturate the QIE in order to test the full range of the QIE. In addition we determined whether the neutral density filter has any effect on the linearity test measurement. We put a reducing factor of $10^{1.2}$ neutral density filter in front of the Reference Pin-Diode to test such effect. Figure 11 shows the result. We conclude there is no such effect.

We test the effect of the wave-shifter on the linearity of our system. We build a small diameter wave-shifting bar out of BBQ. This small width bar can be put against the Test Pin Diode with most of the captured shifted light directed at the pin diode. We set the fixed filter wheels to have no neutral density filter between the vial and the fiber. Figure 12 shows the Reference Pin Diode vs the light at the end of the BBQ in the Black Box. There is no sign of saturation of the BBQ even at the highest light level.

From these studies we conclude our setup optical nonlinearity is less than 0.15% in the full scale range. The deviations shown on Figure 12 are a couple Burr-Brown counts out of 1.05×10^6 counts. These deviations could be due to a differential nonlinearity in the Burr-Brown ADC of $5 \times 10^{-4}\%$.

Table 1: Calibration constant for different tubes.

Tube Type	CEM	CHA	PEM	PHA	WHA
Calibration Constant(MeV/Count)	2.90	2.875	3.68	3.31	2.70

2 PMT Linearity Test

The timing of the apparatus is described in details in Reference [1]. We briefly state it here. The data acquisition systems (DAQ) for the QIE and Burr-Brown ADC are completely separate. The DAQ for the Burr-Brown generates the trigger for the laser. Hence, it is easy to gate the Burr-Brown properly. The QIE has internal clock cycle of 132 ns. We need to time the integration gates properly for both system.

Reference [1] describes the method to select events which have the pulse correctly positioned in the integration gate of the QIE electronics. We try vary the length of the cable so when the laser fires, only those laser signals that start 10-20 ns after the start of the integration in buffer 2 of QIE are selected. For 10 stage tubes(PLUG, CEM, WHA) we set the cable length 88 ns, for 12 stage tubes(CHA) it is 80 ns.

The definition of the nonlinearity in this document is basically the same as the "QIE Linearity Test"[1]. The nonlinearity at the fitted QIE count is the difference between the measured QIE count and the fitted QIE count divided by the fitted QIE count:

$$\text{Nonlinearity(at Q(fit))} = \frac{\text{Q(measure)} - \text{Q(fit)}}{\text{Q(fit)}}$$

The linear calibration matches the ADC outputs at the pedestal and central Z electron point(between 15,000 $\sim$ 17,000 QIE counts), see Figure 13. We also change the QIE count into equivalent energy scale using the calibration constant 2.7$\sim$ 3.68 MeV/Count for different type of tubes. Table 1 lists the calibration constant we use for each type of the tubes.

Since the DAQ limits a run to 1000 events, we usually do a run with 30 steps and 30 firings for each step. Each step is at some certain light level of the tested tube. A

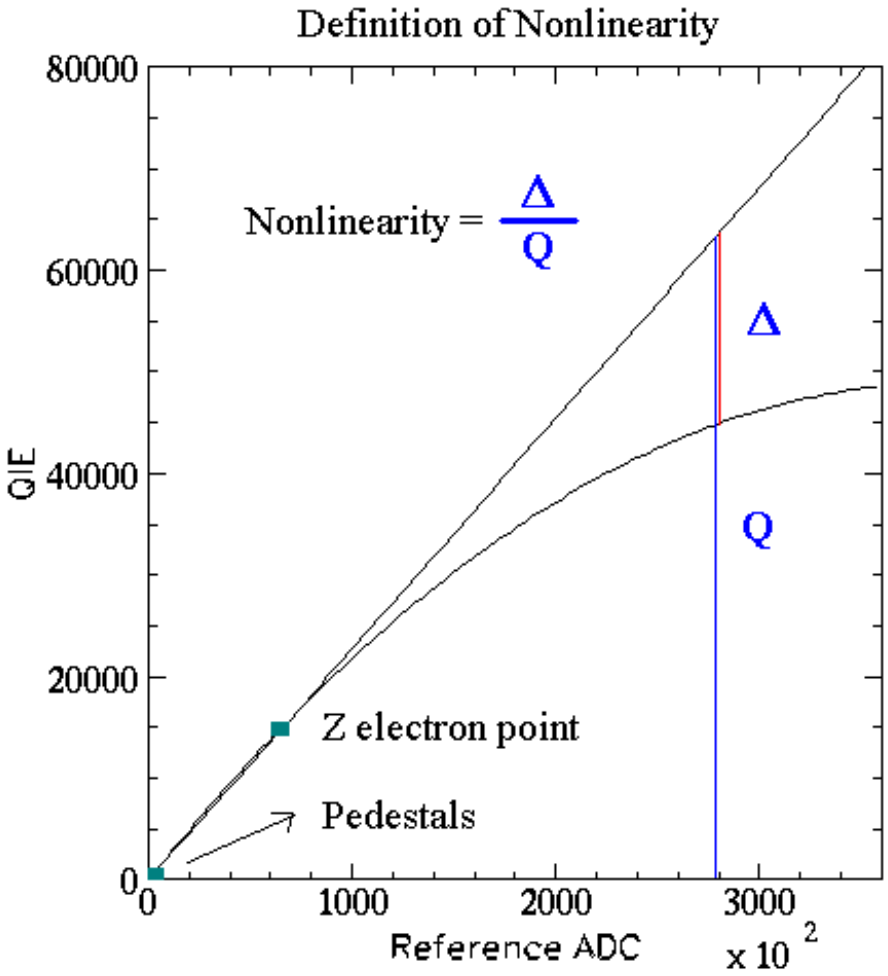

Figure 13: Definition of the nonlinearity. The linear calibration matches the pedestals and the Z electron point.

"full range scan" is a run with the 30 steps distributed evenly over the full range of the tube, and 4 runs makes a good measurement. This takes about half hour. During the "full range scan", the gain is relatively stable because it takes a short time to make a measurement.

The "low range scan" is achieved by putting a neutral density filter before the rotating

filter wheel to study the low end of the tube. For the "low range scan", the ratio of the read out between the Reference Pin-Diode and the tested tube is the same as the "full range scan" as long as the tested tube's gain does not change. We can apply the same calibration for the "low range scan" as the "full range scan"'s calibration in such case.

For the "low range scan", because of the photon statistics, we have to do many more runs, and it takes hours to finish it. Throughout the PMT linearity test, we do not control the temperature of the Black Box, so the temperature varies and the gains of the tube change. Because of the long time the "low range scan" takes, the room temperature changes and affects the gain of the tube. This makes the calibration slightly different from the previous run. We also do the "single point measurement", which fires the laser at certain light level with only 1 step (instead of 30 steps) and with several runs. "Single point measurement" has good statistics, but the gains of the tube may change since the measurement also takes long time. By understanding the temperature change in our room, we conclude the calibration difference caused by the gain change is less than 1%. Hence, we assign 1% systematic error to the low end study which we do not apply in the plots.

Figure 14 shows the voltage distributions for all the tubes and the tubes we tested. We pick the tube for each type randomly, but tried to have the tube voltages span the voltage distributions.

The difference between pseudo pedestal and laser pedestal does not affect the full range study, but it affects the low end study. We pick one or two typical tubes of each type and study the low end as well as the difference between pseudo pedestal and laser pedestal for this tube. We use this difference to adjust the pedestals for all the same type tubes.

The PEM and PHA tubes are the same kind of tubes except at different working voltage range. For CHA we put a LED in the Black Box. We shine the LED with a DC current to stabilize the gain of the tube. The current to the LED is set so that the CHA tube has a DC current of 250 nA.

The WHA tubes have no zener diodes for Run II. During the time we were testing these tubes the WHA bases were suppose to have zener diodes for Run II. Hence we tested the WHA tubes with zener diodes in the base. We measured the difference between WHA tube with and without zeners in the base. That difference is show in figure 15.

The following subsections are the plots show the test results for PEM, PHA, CEM, CHA and WHA. We tested 10 CEM tubes, 9 CHA tubes, 9 WHA tubes, 3 PEM tubes and 3 PHA tubes with high voltages on the plots. We put all the tubes of one type in a

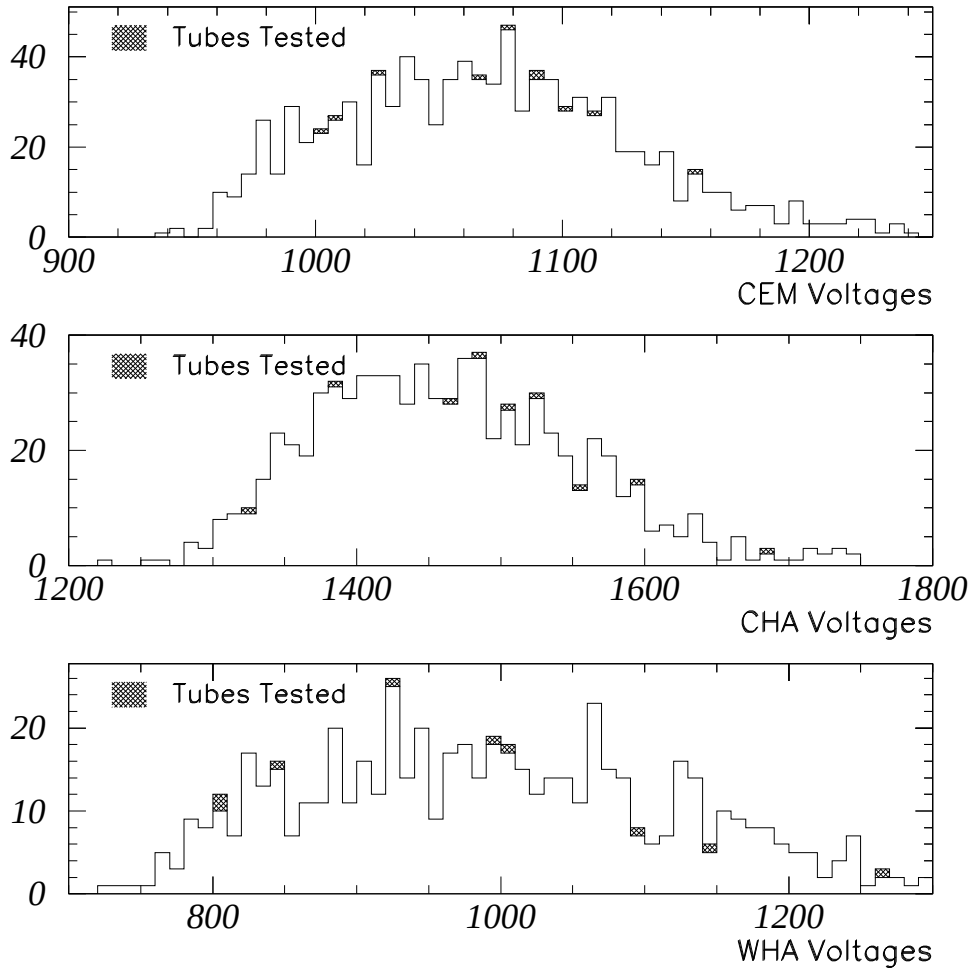

Figure 14: Voltage distributions for different tubes. The voltages tested are also show on the plot.

plot. In addition to make the central tubes and wall hadron tube's data easier to see, we put 3-4 tubes in a plot. For each type of the tube, we studied one tube for the low end in details. All the plots are for buffer 2 only.

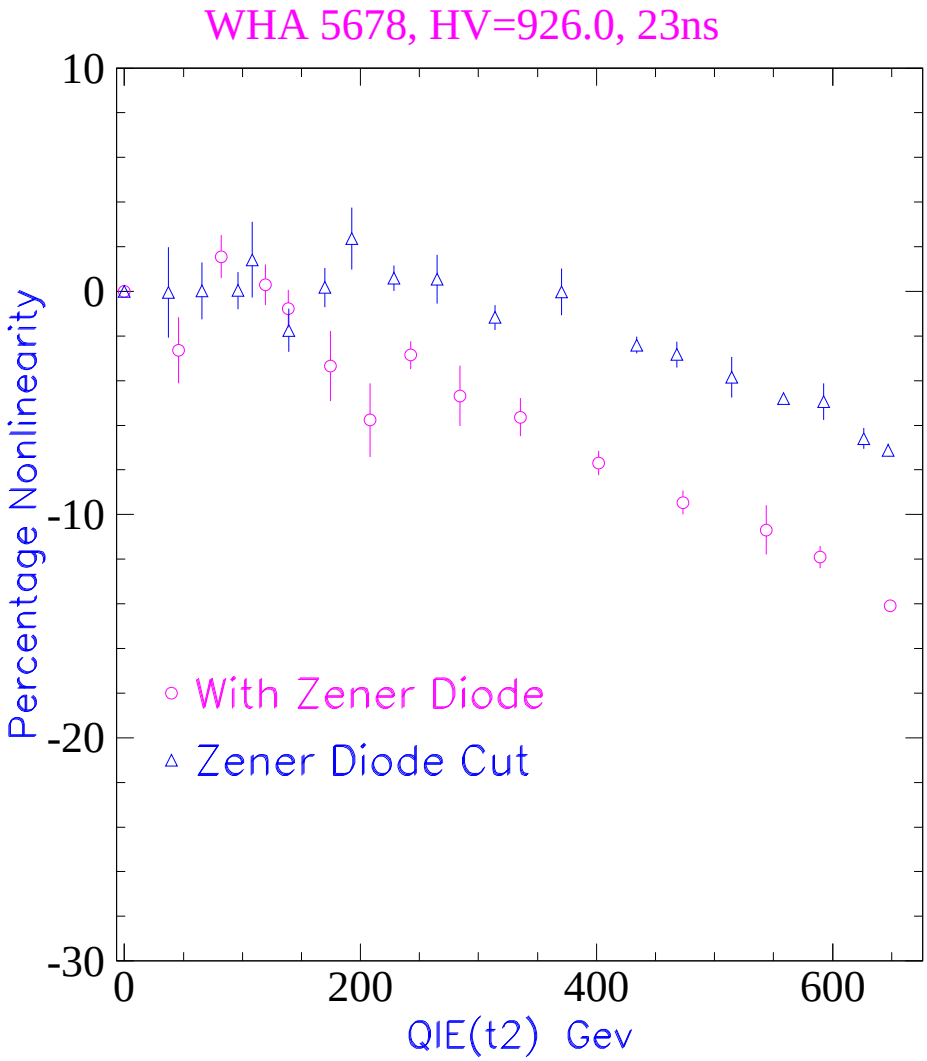

Figure 15: One WHA tube linearity with and without Zener Diode. The one with Zener Diode cut is better than the one with Zener Diode there.

2.1 PEM tubes

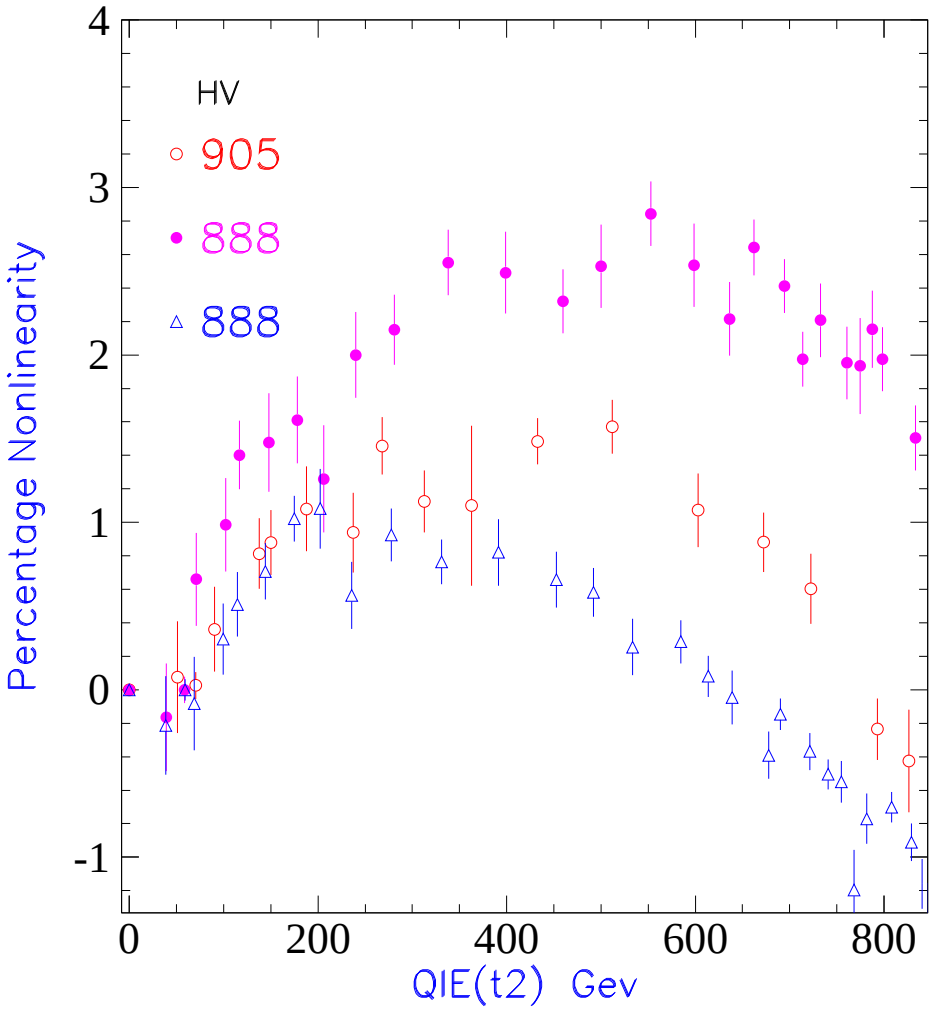

Figure 16: PEM tubes nonlinearity. All the three tested PEM tubes are overlayed in one plot. The high voltage for the tubes is shown on the plot. Only QIE buffer 2 which has the most deposited energy are tested.

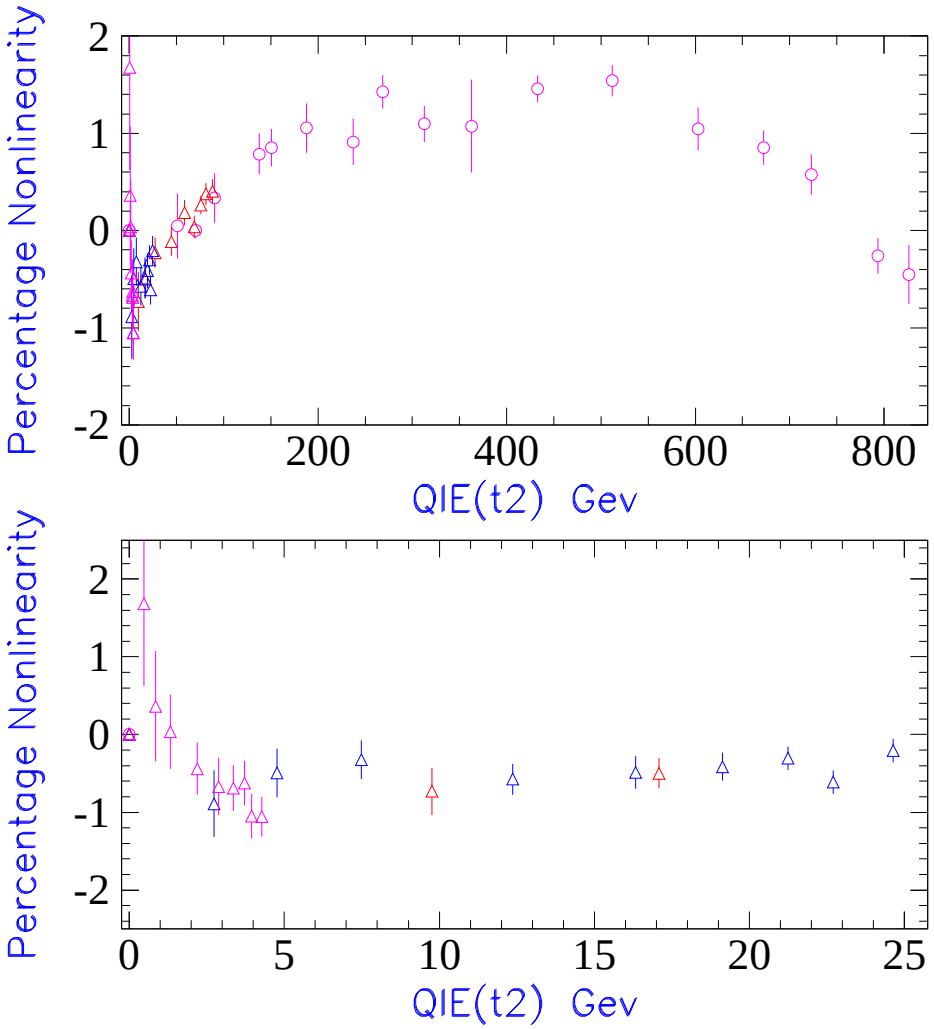

Figure 17: PEM tubes nonlinearity at low range. The data for this figure comes from the tube with HV = 905.

2.2 PHA tubes

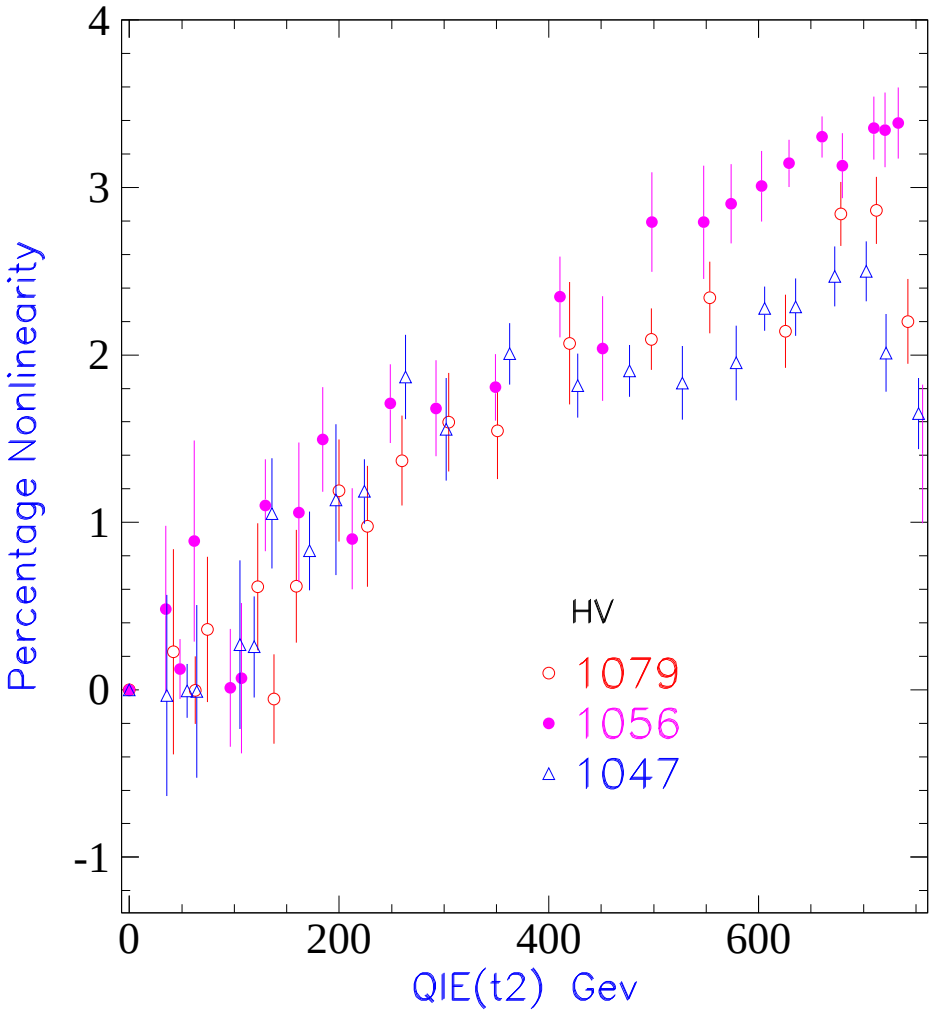

Figure 18: PHA tubes nonlinearity

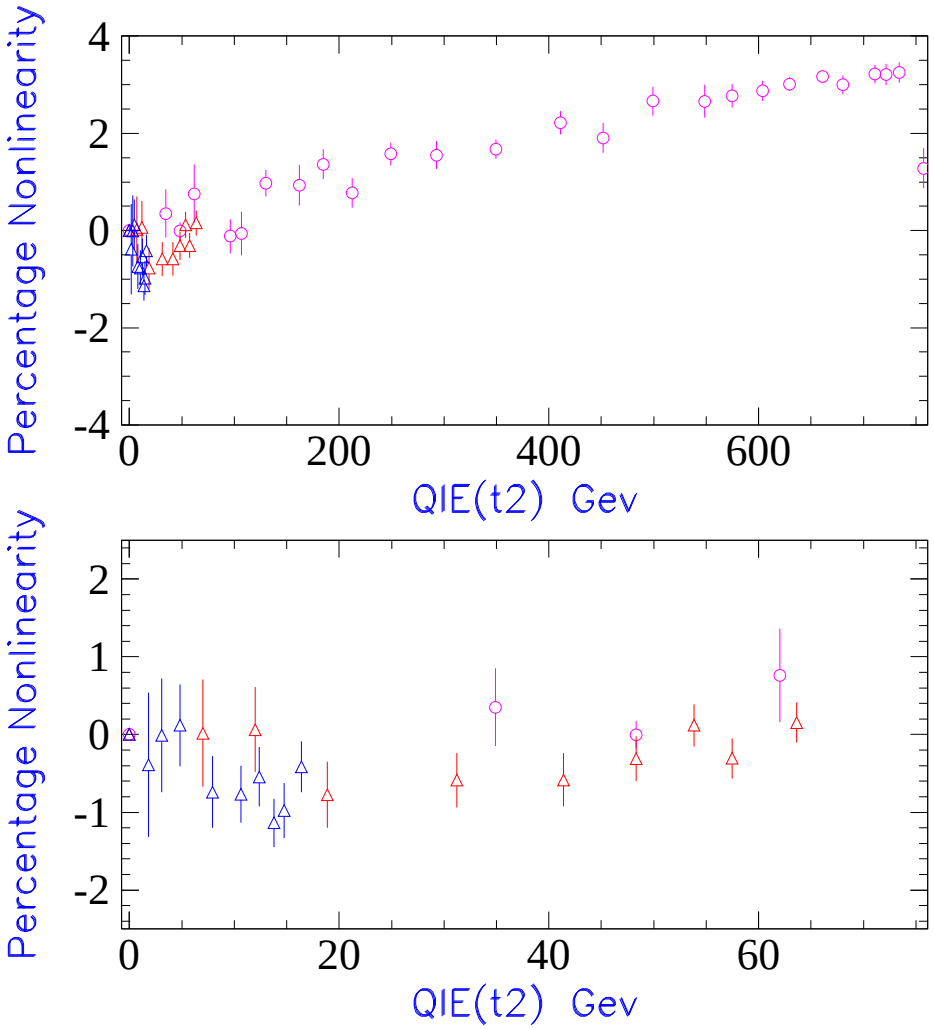

Figure 19: PHA tubes nonlinearity at low range. The data for this figure comes from the tube with HV = 1056.

2.3 CEM tubes

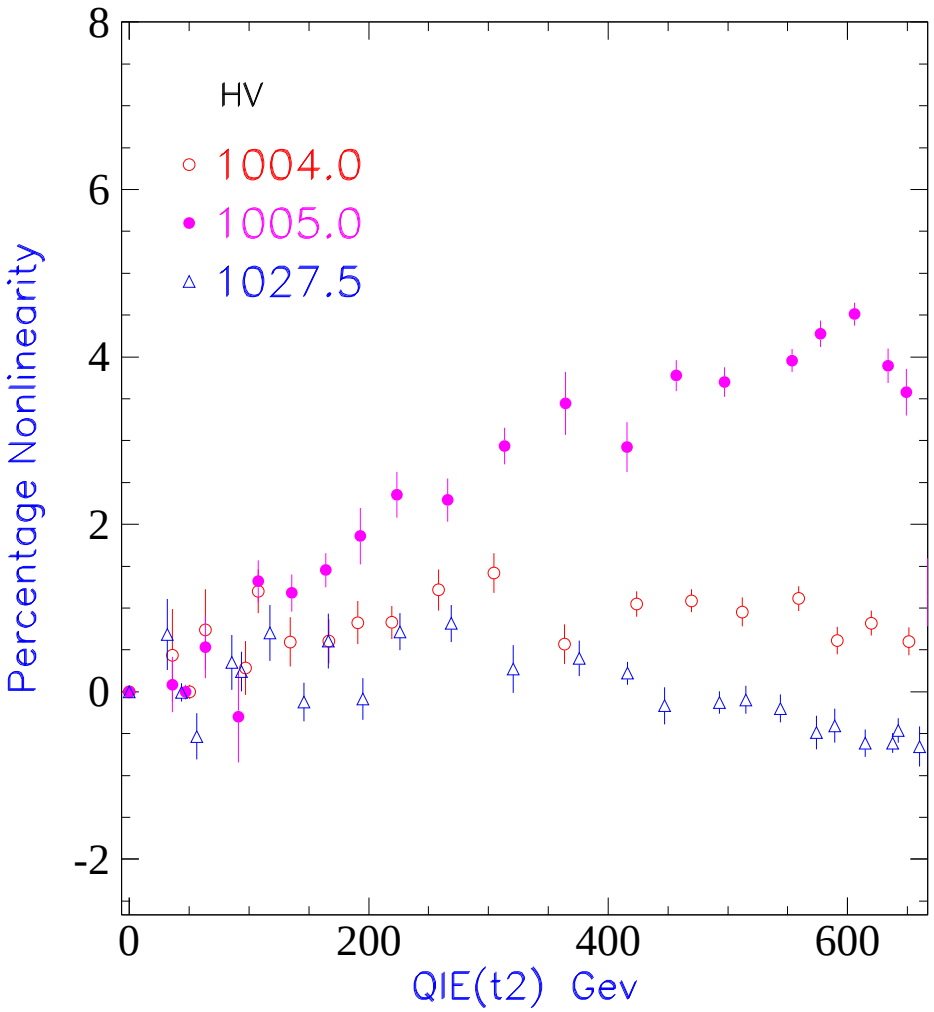

Figure 20: CEM tubes nonlinearity. Three of the tested CEM tubes are overlayed in one plot.Only QIE buffer 2 which has the most deposited energy are tested.

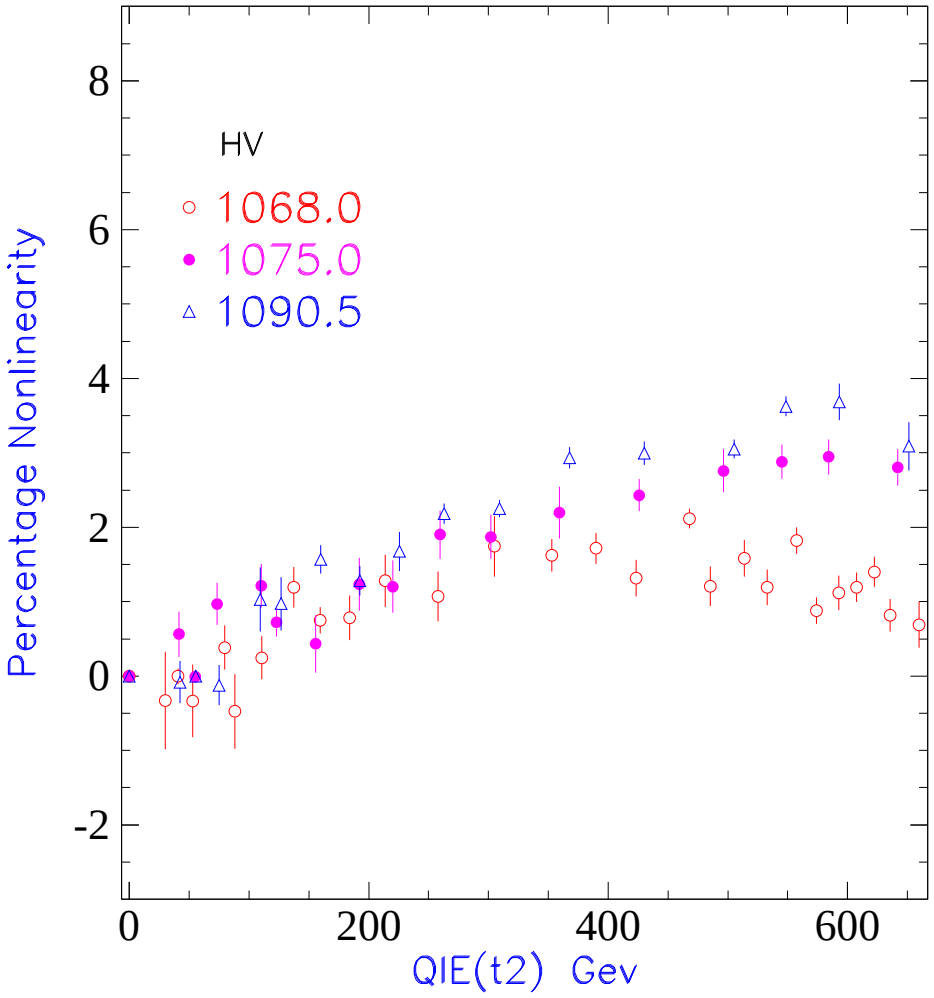

Figure 21: CEM tubes nonlinearity

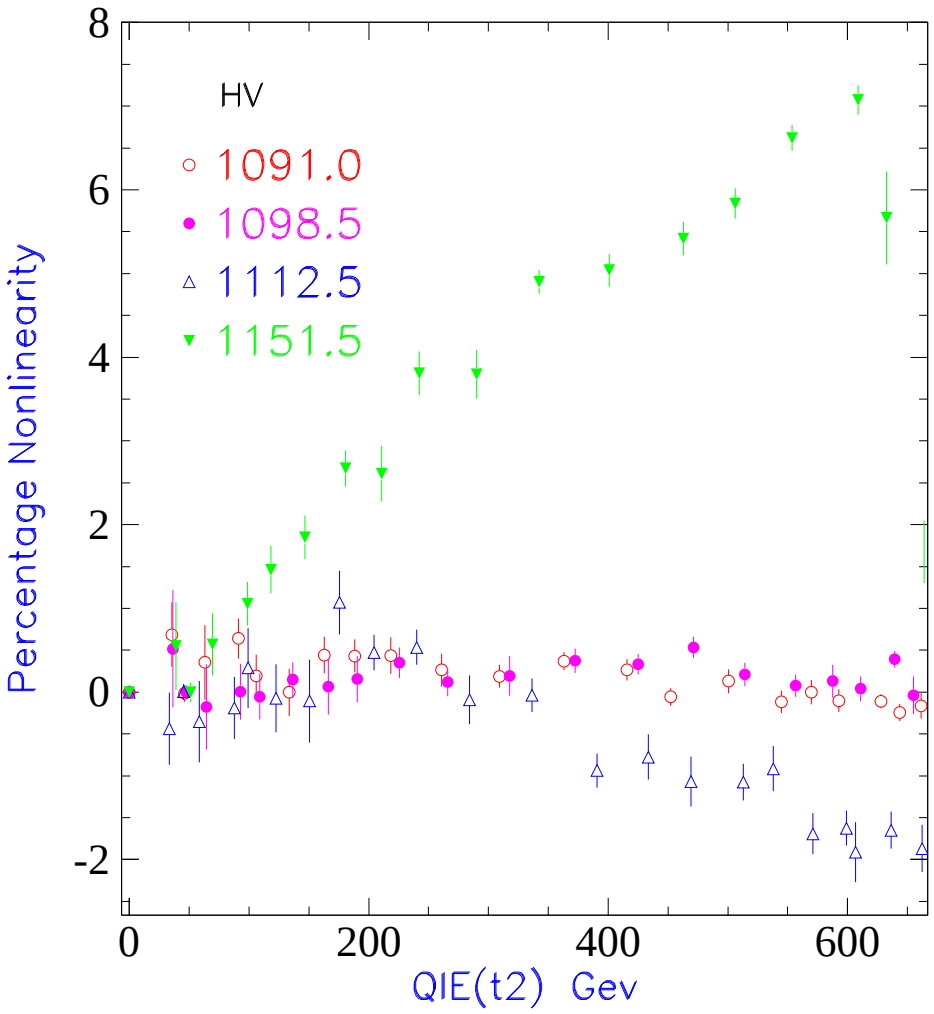

Figure 22: CEM tubes nonlinearity

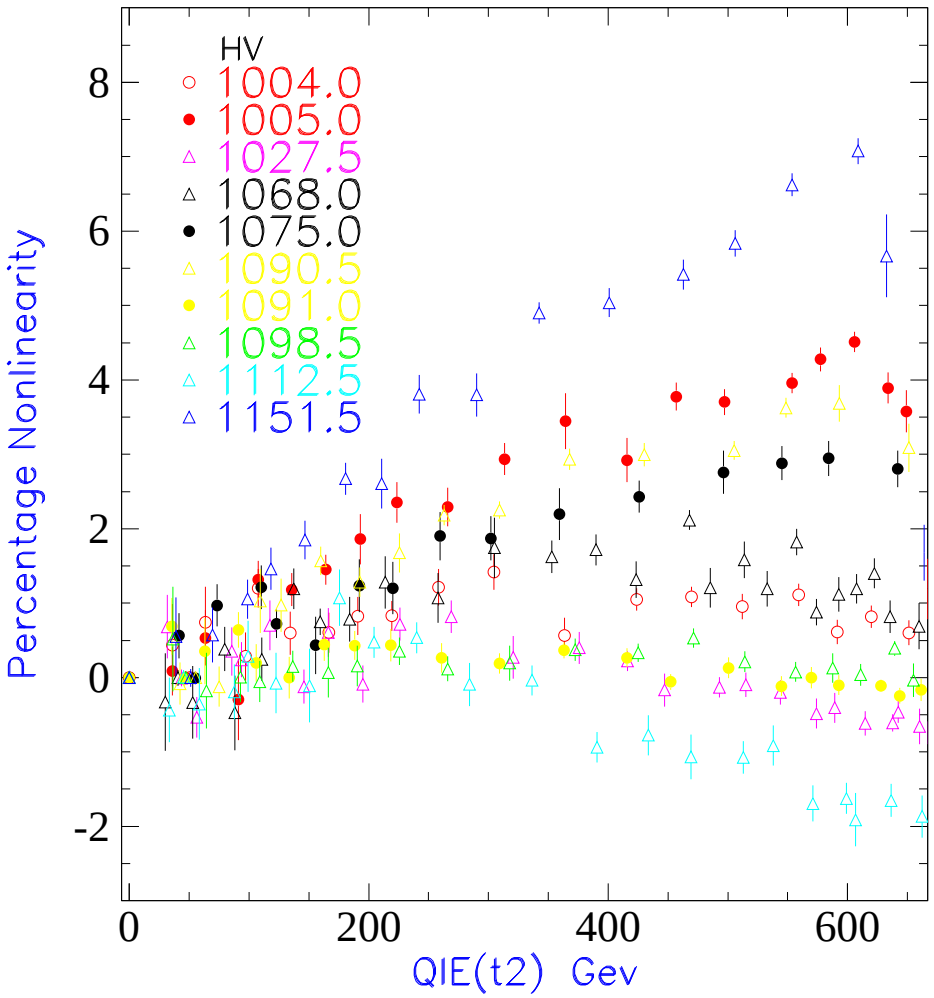

Figure 23: CEM tubes nonlinearity. All the tested CEM tubes are overlayed in one plot. Only QIE buffer 2 which has the most deposited energy are tested.

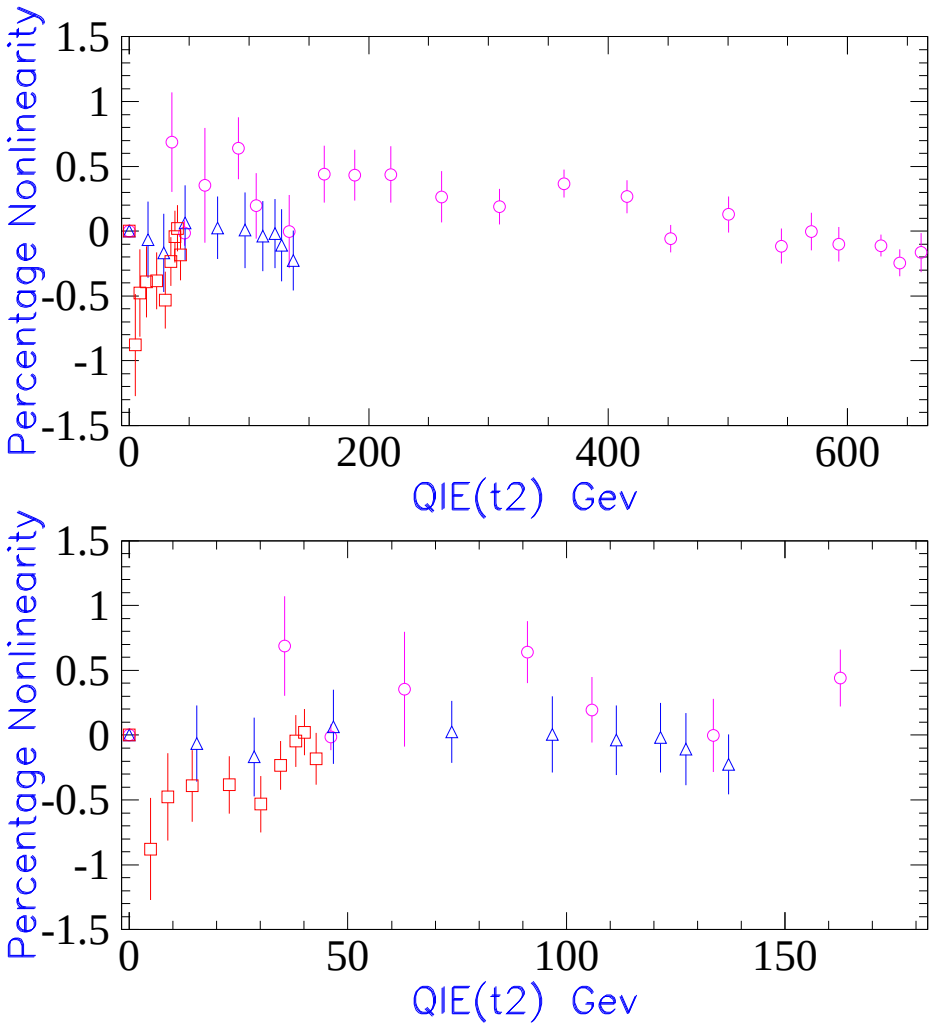

Figure 24: CEM tube 22E 6R nonlinearity. Only QIE buffer 2 which has the most deposited energy are tested. The low end of this tube is also tested. The data for this figure comes from the tube with HV = 1091.0

2.4 CHA tubes

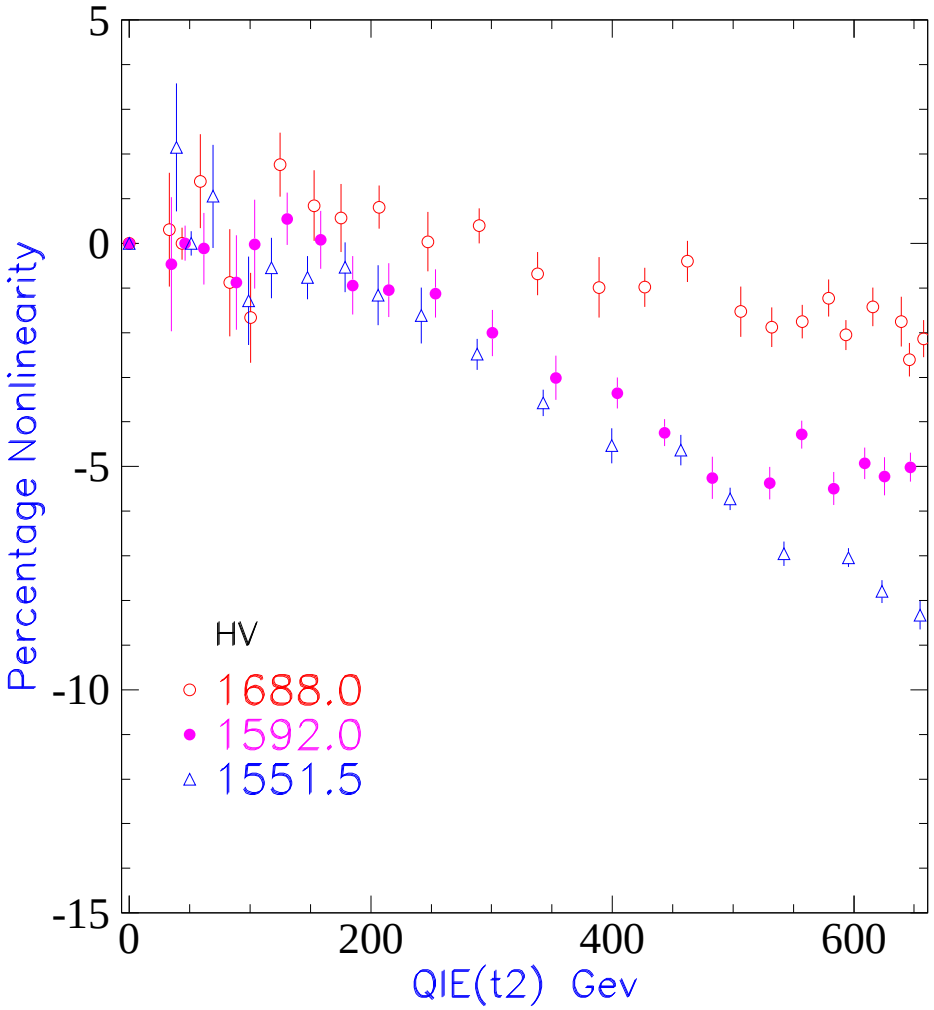

Figure 25: CHA tubes nonlinearity.

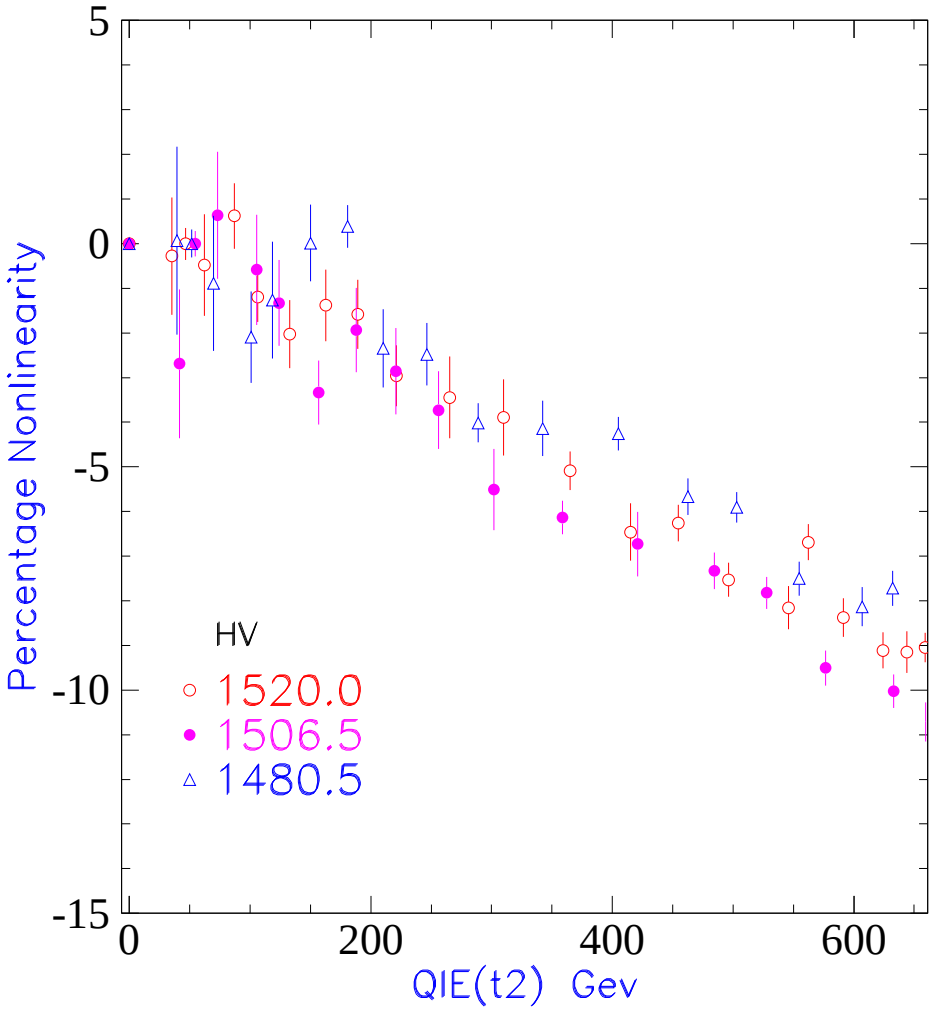

Figure 26: CHA tubes nonlinearity.

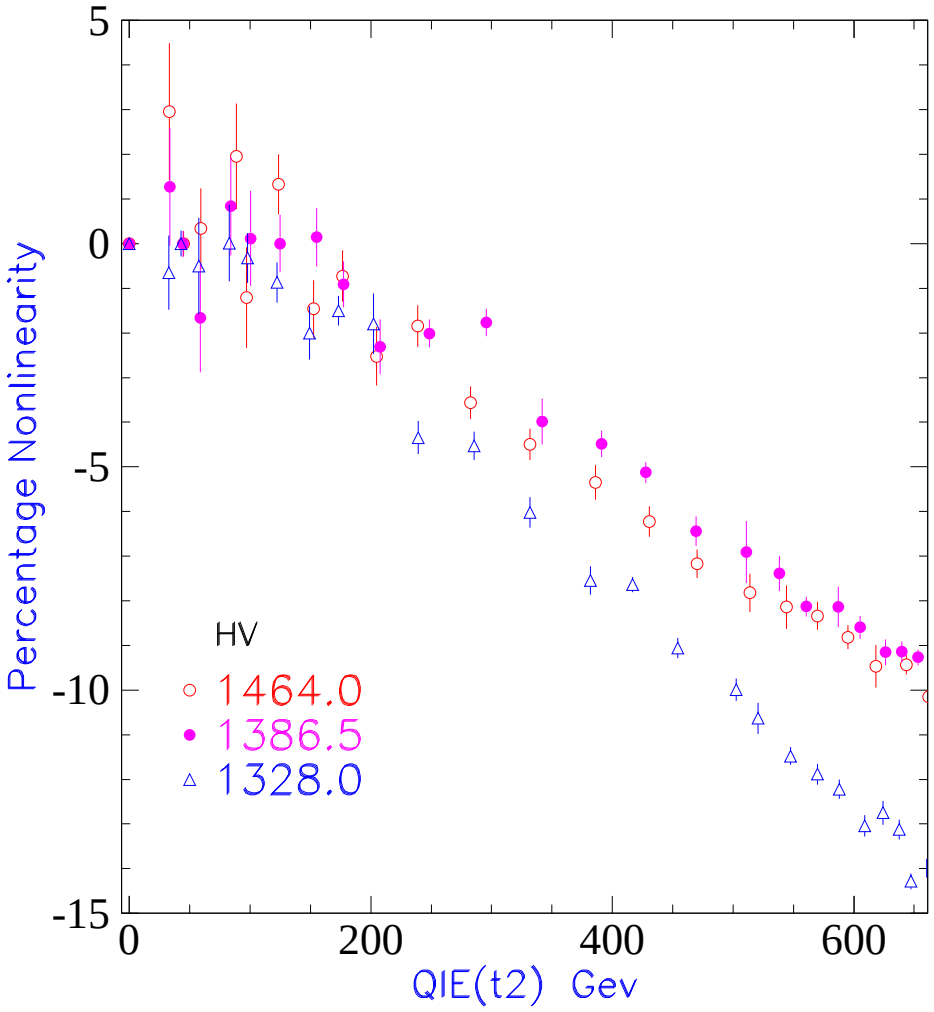

Figure 27: CHA tubes nonlinearity.

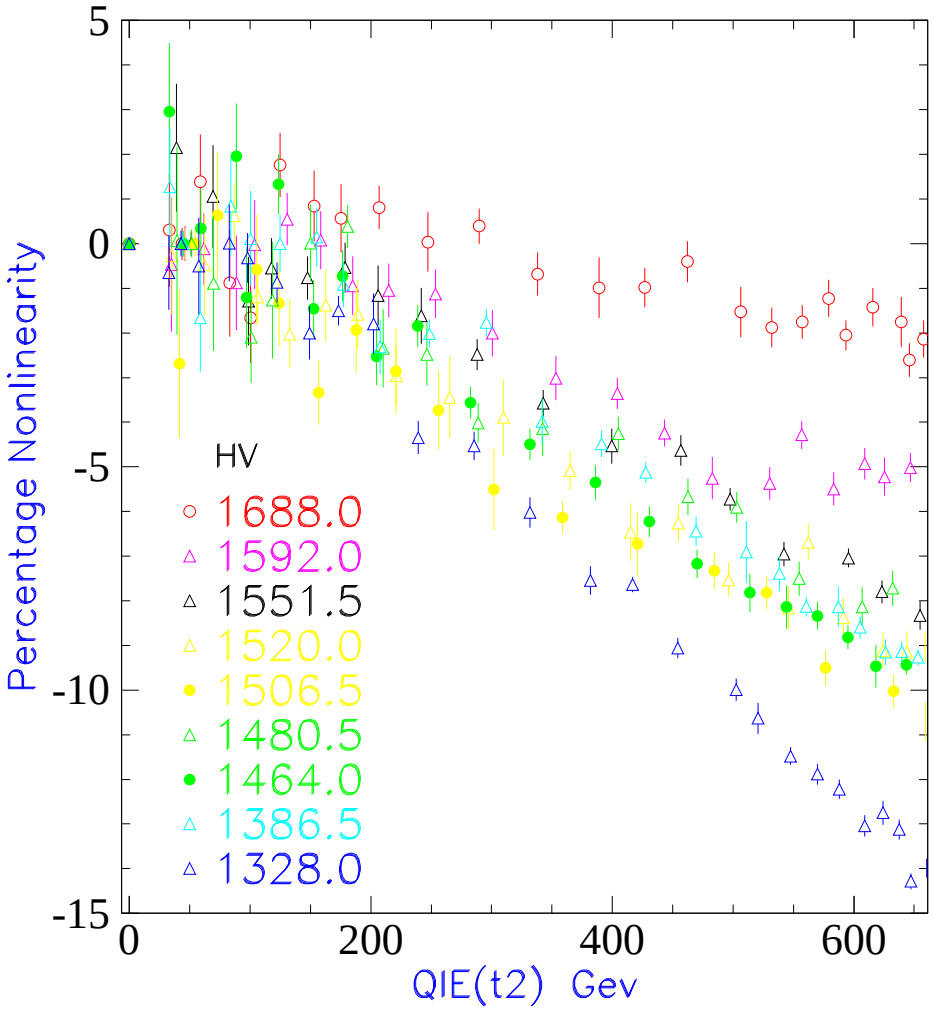

Figure 28: CHA tubes nonlinearity in one plot.

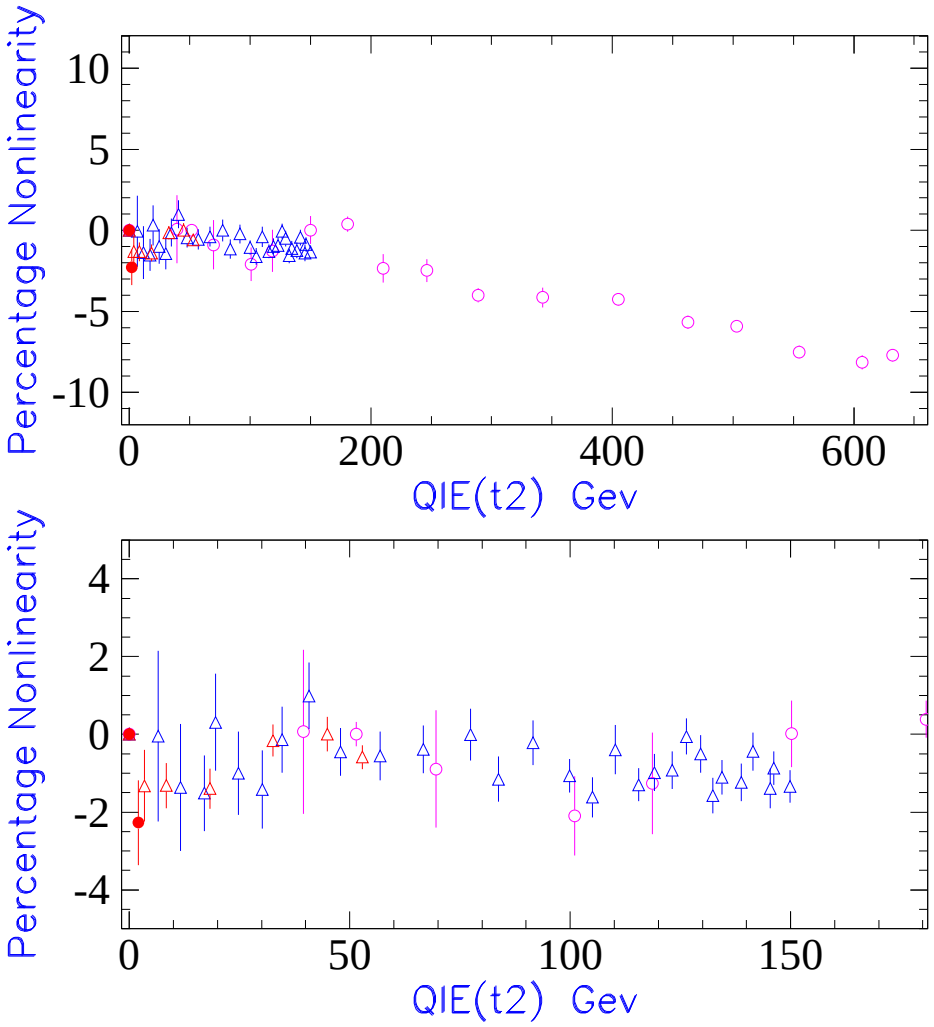

Figure 29: CHA tubes nonlinearity at low range. The data for this figure comes from the tube with HV = 1480.5. The solid bullet other than the one at 0 is a "single point measurement" with better statistics.

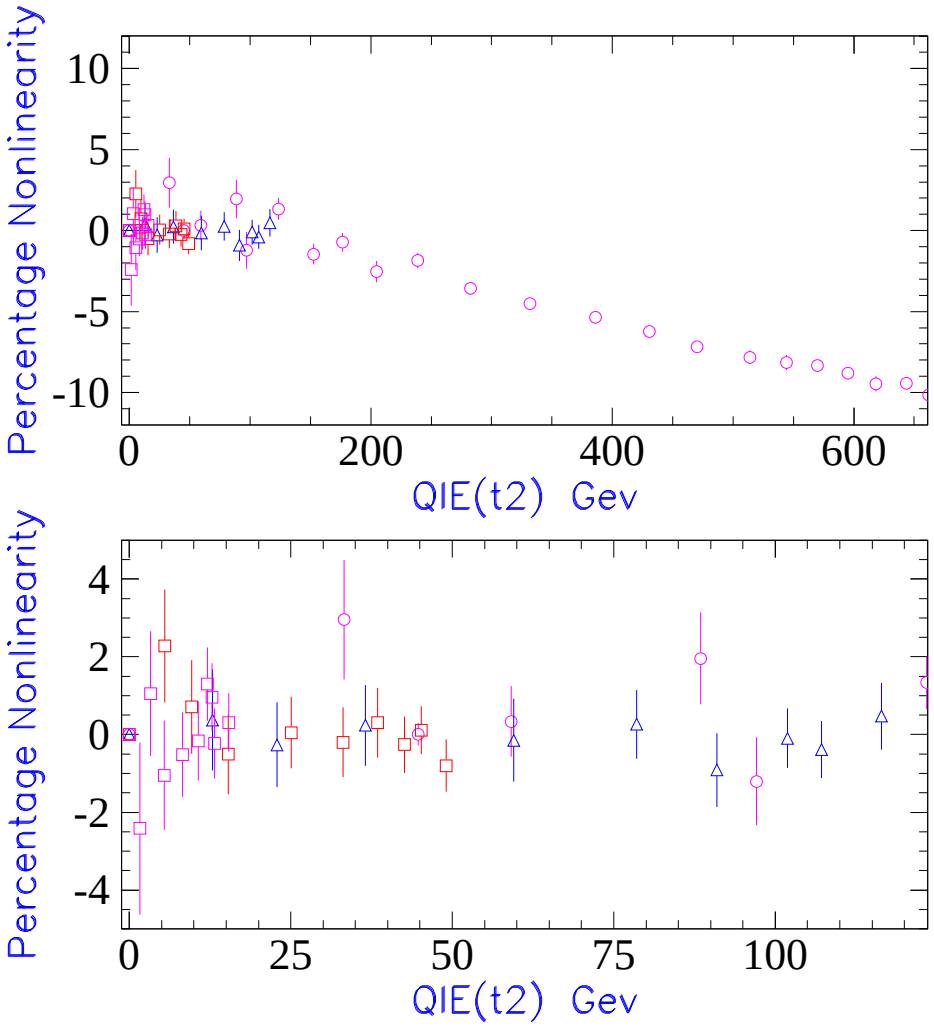

Figure 30: CHA tubes nonlinearity at low range. The data for this figure comes from the tube with HV = 1464.0

2.5 WHA tubes

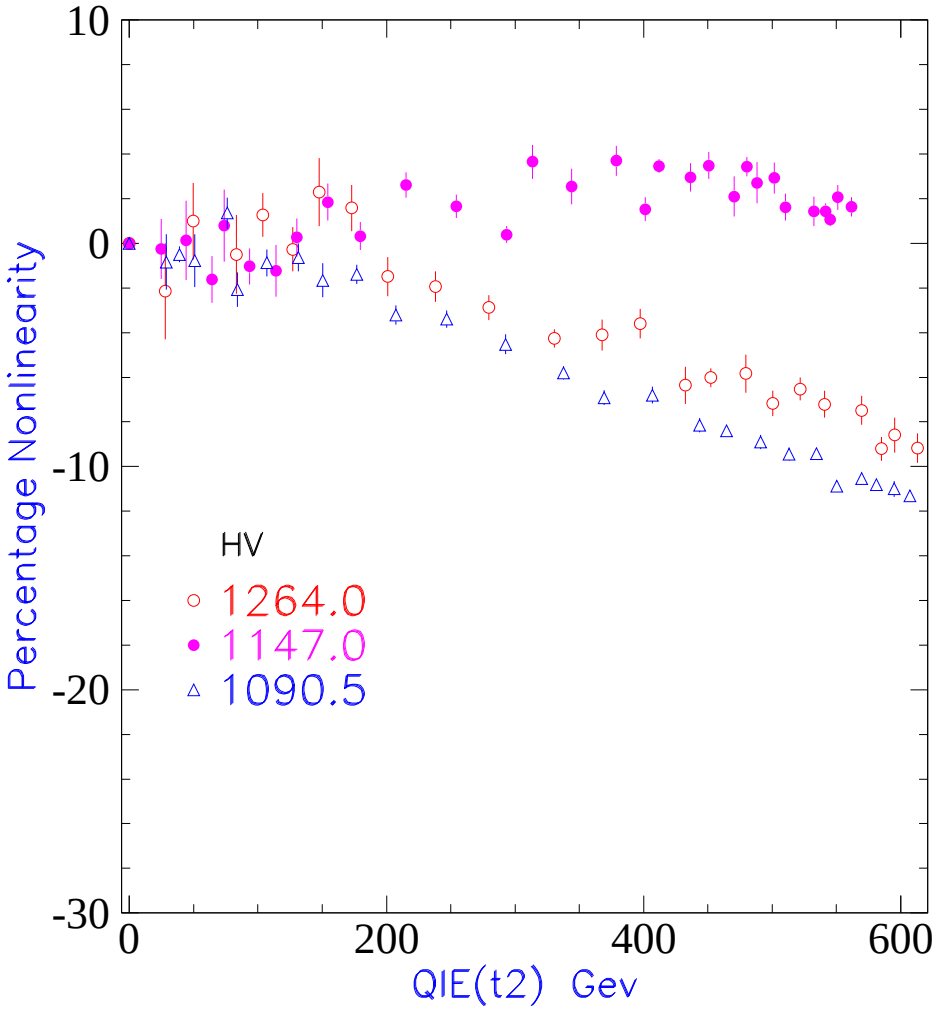

Figure 31: WHA tubes nonlinearity

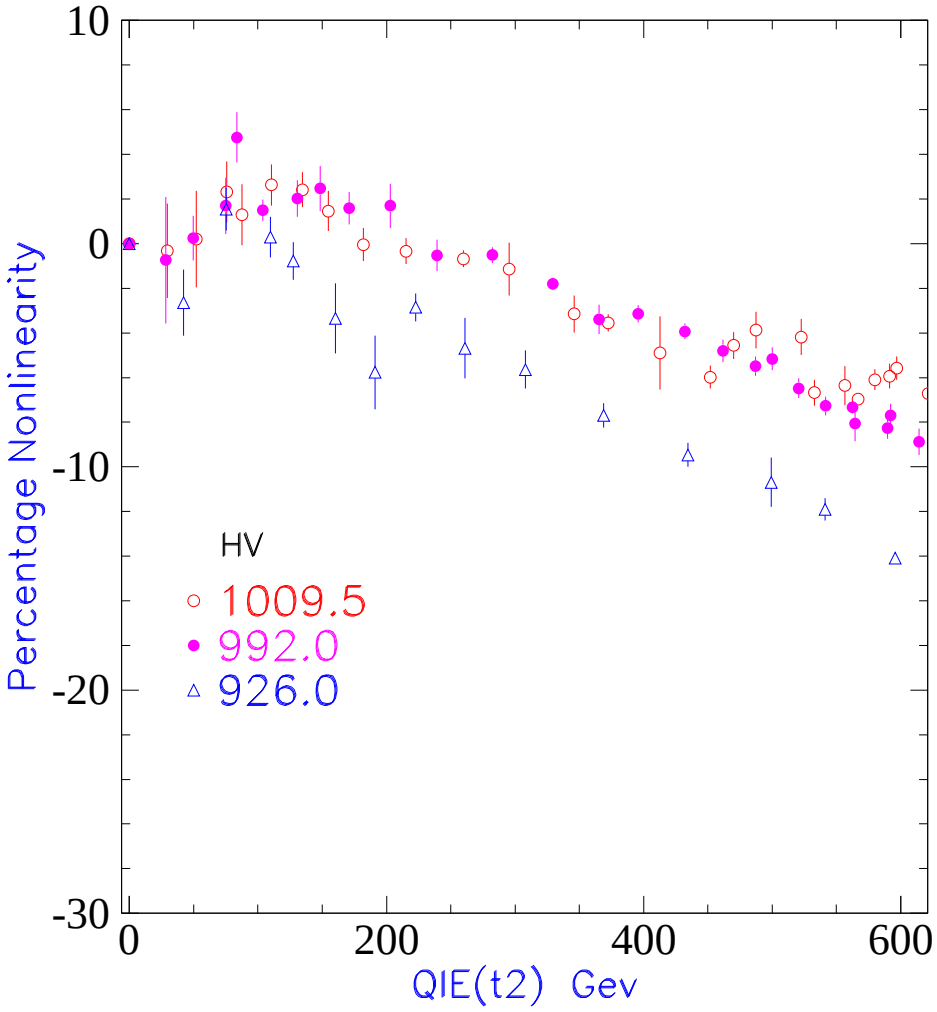

Figure 32: WHA tubes nonlinearity

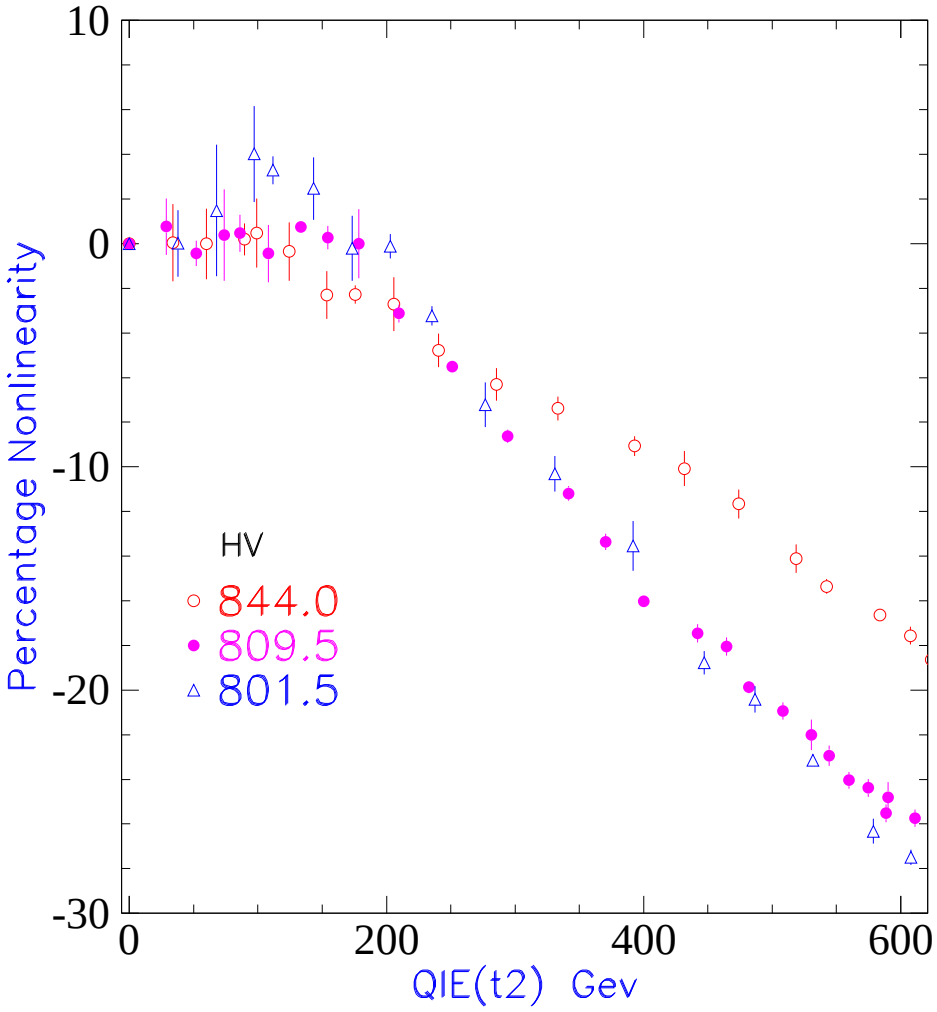

Figure 33: WHA tubes nonlinearity

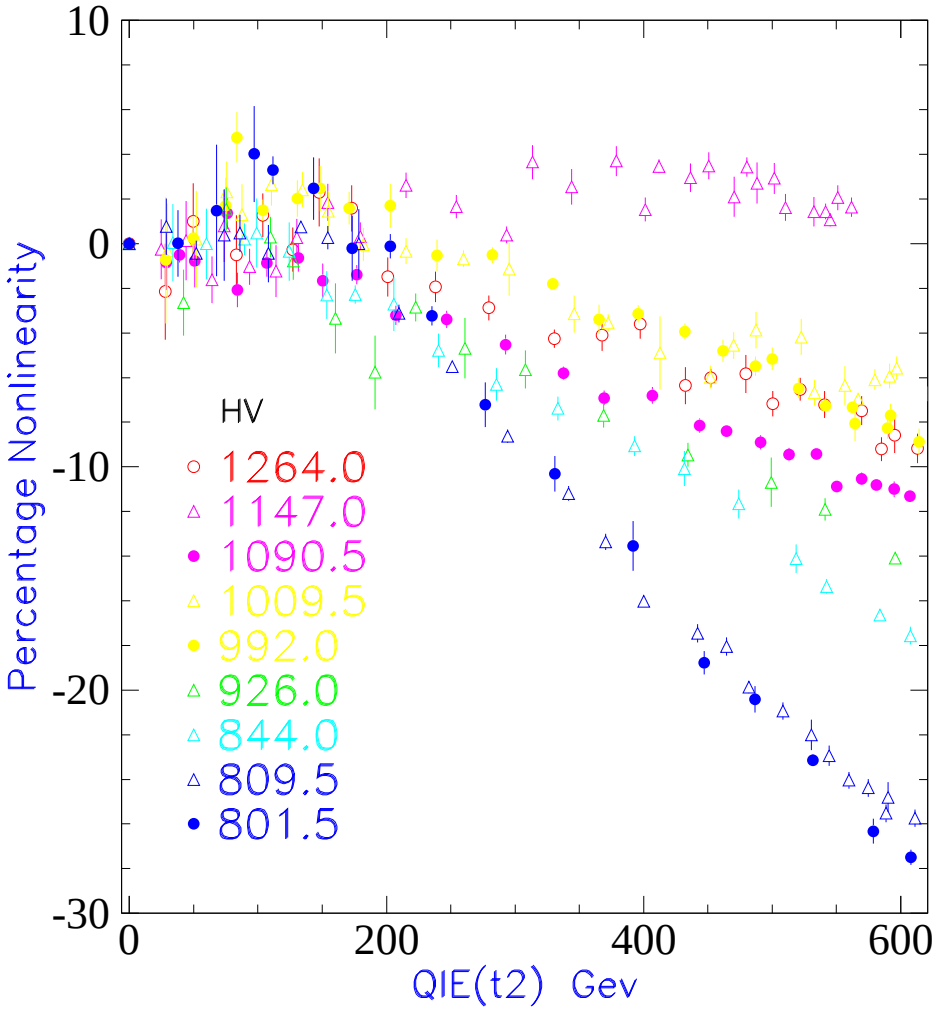

Figure 34: WHA tubes nonlinearity in one plot

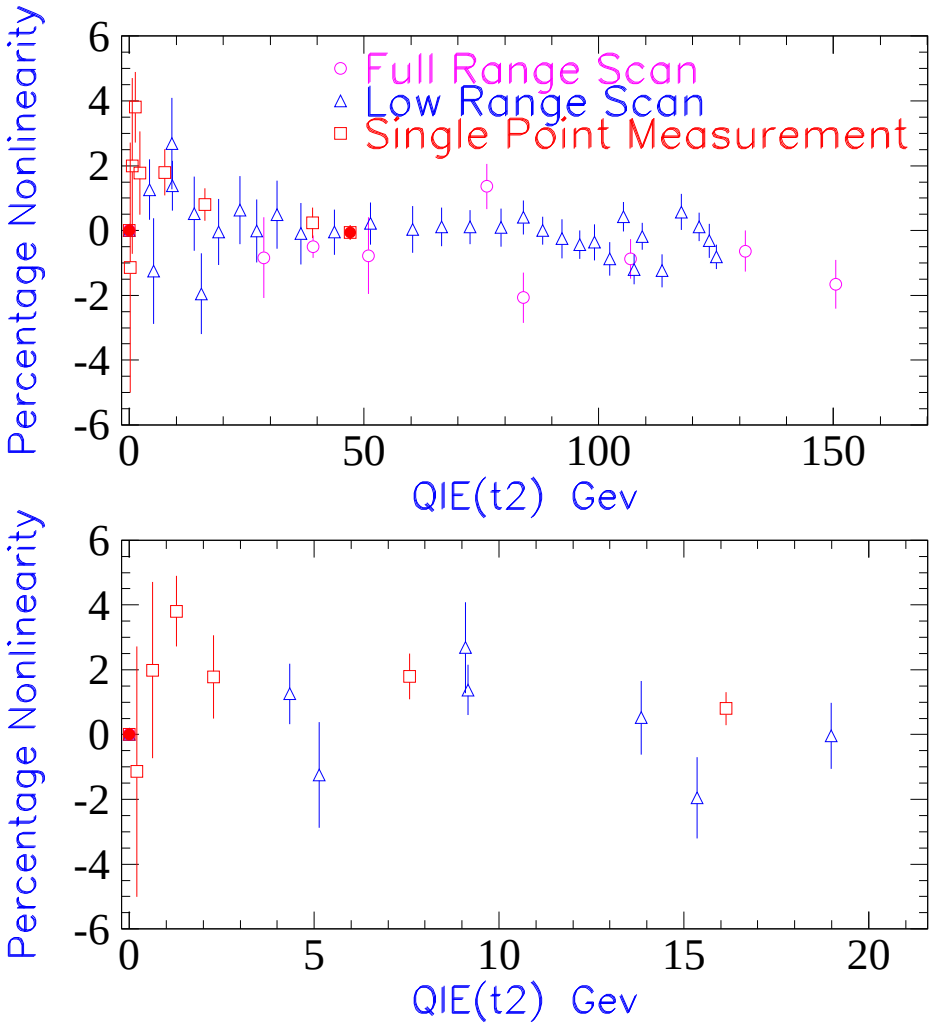

Figure 35: WHA tubes nonlinearity at low range. The data for this figure comes from the tube with HV = 1090.5

3 Conclusion

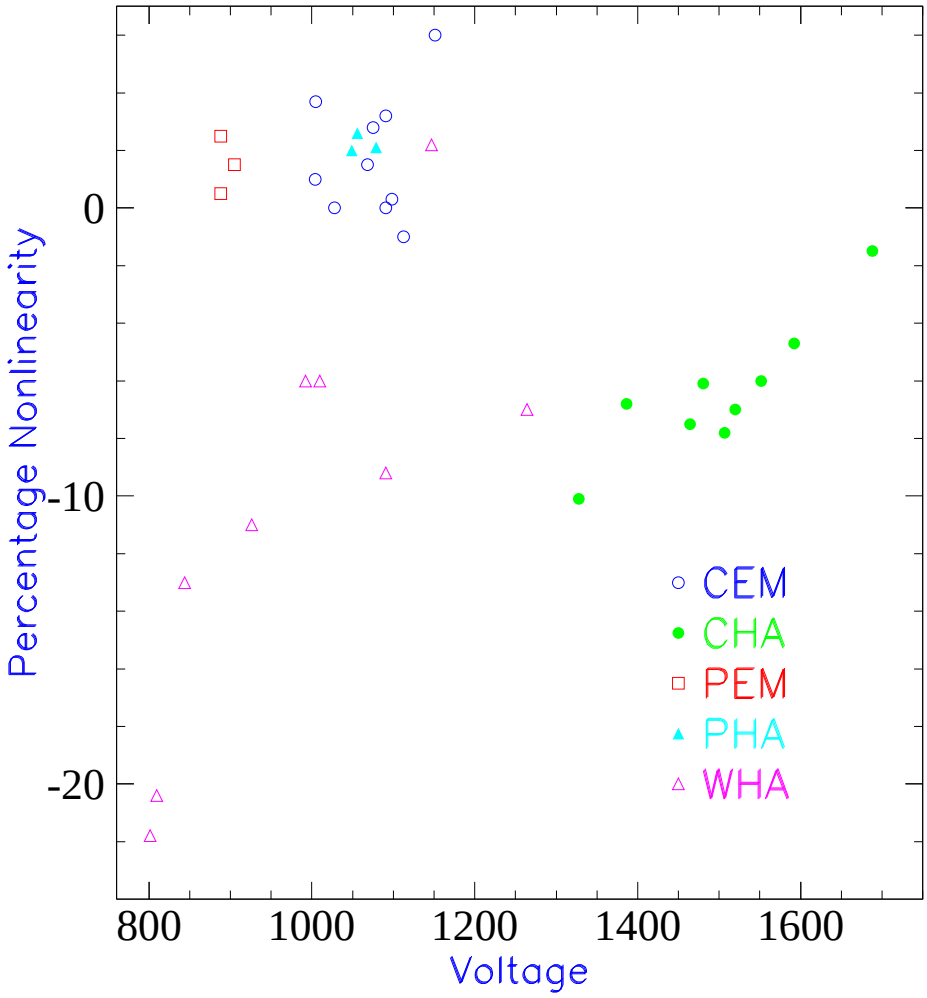

Figure 36: Percentage of the Nonlinearity vs High Voltage for CEM, CHA, PEM, PHA and WHA tubes at 500 GeV

The dependence of the nonlinearity for each type of the tube on the working voltage is shown in figure 36. Table 2 gives the nonlinearity of the tubes. For the CHA and WHA

Table 2: Nonlinearity of different tubes. The first row is the equivalent energy scale for the QIE full range. The second row is the percentage nonlinearity for the range with the deposited energy less than 20 GeV. The third row is the percentage nonlinearity for the range with the deposited energy less than 200 GeV. The fourth row is the percentage nonlinearity for the full range energy scale.

Type	PEM	PHA	CEM	CHA	WHA
energy range (GeV)	850	760	660	660	620
% nonlinearity($<$ 20 GeV)	1.5	1.5	1.0	2.0	4.0
% nonlinearity($<$ 200 GeV)	2.0	1.5	3.0	4.0	6.0
% nonlinearity(full range)	3.0	3.5	7.0	15	28

tubes, we see the nonlinearity varies as a function of the working voltage. For the CEM and PLUG tubes, we do not see the variations in the nonlinearity as a function of the working voltage.

In addition, we have two separate ASCII files for the complete data information for both buffer 2 only and sum of buffer 2 and buffer 3.

4 Appendix

The ASCII files for the data shown in these plots are on the CDF public code area

http://cdfcodebrowser.fnal.gov/CdfCode/source/Calor/doc/
pmttest_data_t2.txt
pmttest_data_t23.txt

These data are given in terms of Burr-Brown counts and QIE counts with no ADC count to GeV calibration.

References

[1] H. Budd, M. Lindgren and H. Niu, "QIE Linearity Test." CDF5188.

[2] LINUX IEEE CAMAC library for the Jorway 411S SCSI CAMAC Driver and the Jorway 73A SCSI CAMAC Crate Controller. J.Streets and D.Slimmer, PN540

[3] 20-BIT ANALOG-TO-DIGITAL CONVERTER, Burr-Brown Corporation, PDS-1 211A.

[4] T. Zimmerman, M. Sarraj, "A Second Generation Charge Integrator and Encoder ASIC", IEEE Transactions on Nuclear Science, Vol. 43, No. 3, June, 1996, pp. 1683-1688

[5] H. Budd and M. Lindgren "Endplug Calorimeter Testbeam PMT pulse shapes" CDF5451 .